NAVAL POSTGRADUATE SCHOOL

MONTEREY, CALIFORNIA

THESIS

CLOUD PHASE AND THE SURFACE ENERGY BALANCE OF THE ARCTIC: AN INVESTIGATION OF MIXED-PHASE CLOUDS

by

Kristopher J. Kripchak

March 2008

Thesis Advisor:	Peter Guest
Second Reader:	Tom Murphree

Approved for public release; distribution is unlimited

THIS PAGE INTENTIONALLY LEFT BLANK

REPORT DOCUMENTATION PAGE			Form Approved OMB No. 0704-0188
Public reporting burden for this collection of information is estimated to average 1 hour per response, including the time for reviewing instruction, searching existing data sources, gathering and maintaining the data needed, and completing and reviewing the collection of information. Send comments regarding this burden estimate or any other aspect of this collection of information, including suggestions for reducing this burden, to Washington headquarters Services, Directorate for Information Operations and Reports, 1215 Jefferson Davis Highway, Suite 1204, Arlington, VA 22202-4302, and to the Office of Management and Budget, Paperwork Reduction Project (0704-0188) Washington DC 20503.			
1. AGENCY USE ONLY ***(Leave blank)***	**2. REPORT DATE** March 2008	**3. REPORT TYPE AND DATES COVERED** Master's Thesis	
4. TITLE AND SUBTITLE Cloud Phase and the Surface Energy Balance of the Arctic; An Investigation of Mixed-Phase Clouds		**5. FUNDING NUMBERS**	
6. AUTHOR(S) Kripchak, Kristopher J.			
7. PERFORMING ORGANIZATION NAME(S) AND ADDRESS(ES) Naval Postgraduate School Monterey, CA 93943-5000		**8. PERFORMING ORGANIZATION REPORT NUMBER**	
9. SPONSORING /MONITORING AGENCY NAME(S) AND ADDRESS(ES) N/A		**10. SPONSORING/MONITORING AGENCY REPORT NUMBER**	
11. SUPPLEMENTARY NOTES The views expressed in this thesis are those of the author and do not reflect the official policy or position of the Department of Defense or the U.S. Government.			
12a. DISTRIBUTION / AVAILABILITY STATEMENT Approved for public release; distribution is unlimited.		**12b. DISTRIBUTION CODE**	

13. ABSTRACT (maximum 200 words)

This study examines the phase relationship (liquid versus ice) in Arctic clouds Although it is recognized that clouds are fundamental components of the surface energy balance, the nature of Arctic cloud phase is poorly understood and may have important implications for feedbacks associated with the rapid disappearance of sea ice. This study uses the annual cycle of cloud, radiation, and meteorological measurements made as part of the Surface Heat Budget of the Arctic Ocean field program to derive empirical relationships for cloud liquid fraction as a function of observed variables. Relative to each other, single-layer liquid, ice, and mixed-phase clouds occurred 17.6%, 39.4%, and 42.9% of the time, respectively. The dominant role that mixed-phase clouds play in the surface energy balance of the Arctic was confirmed, emphasizing the need for their correct parameterization in models at all scales. A linear fit of liquid fraction to cloud base temperature between -36^{o}C and +2^{o}C predicts 35% of the fraction variance. Including the observed variables of cloud base height and surface wind speed as predictors predicts another 10%.

14. SUBJECT TERMS SHEBA, Polar Meteorology, Sea Ice, Mixed-Phase Clouds, Arctic Surface Energy Balance, Cloud Parameterization			**15. NUMBER OF PAGES** 83
			16. PRICE CODE
17. SECURITY CLASSIFICATION OF REPORT Unclassified	**18. SECURITY CLASSIFICATION OF THIS PAGE** Unclassified	**19. SECURITY CLASSIFICATION OF ABSTRACT** Unclassified	**20. LIMITATION OF ABSTRACT** UU

NSN 7540-01-280-5500 Standard Form 298 (Rev. 2-89)
Prescribed by ANSI Std. 239-18

THIS PAGE INTENTIONALLY LEFT BLANK

Approved for public release; distribution is unlimited

CLOUD PHASE AND THE SURFACE ENERGY BALANCE OF THE ARCTIC: AN INVESTIGATION OF MIXED-PHASE CLOUDS

Kristopher J. Kripchak
Captain, United States Air Force
B.S. Physics, The University of Akron, 2000

Submitted in partial fulfillment of the
requirements for the degree of

MASTER OF SCIENCE IN METEOROLOGY

from the

NAVAL POSTGRADUATE SCHOOL
March 2008

Author: Kristopher J. Kripchak

Approved by: Peter Guest
Thesis Advisor

Tom Murphree
Second Reader

Phil Durkee
Chairman, Department of Meteorology

THIS PAGE INTENTIONALLY LEFT BLANK

ABSTRACT

This study examines the phase relationship (liquid versus ice) in Arctic clouds Although it is recognized that clouds are fundamental components of the surface energy balance, the nature of Arctic cloud phase is poorly understood and may have important implications for feedbacks associated with the rapid disappearance of sea ice. This study uses the annual cycle of cloud, radiation, and meteorological measurements made as part of the Surface Heat Budget of the Arctic Ocean field program to derive empirical relationships for cloud liquid fraction as a function of observed variables. Relative to each other, single-layer liquid, ice, and mixed-phase clouds occurred 17.6%, 39.4%, and 42.9% of the time, respectively. The dominant role that mixed-phase clouds play in the surface energy balance of the Arctic was confirmed, emphasizing the need for their correct parameterization in models at all scales. A linear fit of liquid fraction to cloud base temperature between -36^{o}C and +2^{o}C predicts 35% of the fraction variance. Including the observed variables of cloud base height and surface wind speed as predictors predicts another 10%.

THIS PAGE INTENTIONALLY LEFT BLANK

TABLE OF CONTENTS

LIST OF FIGURES

THIS PAGE INTENTIONALLY LEFT BLANK

LIST OF TABLES

THIS PAGE INTENTIONALLY LEFT BLANK

LIST OF ACRONYMS

AGL	-	Above Ground Level
ASFG	-	Atmospheric Surface Flux Group
CF	-	Cloud Radiative Forcing
CF_{LW}	-	Longwave Cloud Forcing
CF_LW	-	Longwave Cloud Forcing
CF_LWD	-	Longwave Cloud Forcing Down
CF_LWU	-	Longwave Cloud Forcing Up
CF_{SW}	-	Shortwave Cloud Forcing
CF_SW	-	Shortwave Cloud Forcing
CF_SWD	-	Shortwave Cloud Forcing Down
CF_SWU	-	Shortwave Cloud Forcing Up
DISORT SBDART	-	Santa Barbara Discrete Ordinate Radiative Transfer Atmospheric Radiative Transfer algorithm
GPS	-	Global Positioning Satellite
IWP	-	Column Integrated Ice Water Path
LORAN	-	Long Range Navigation
LowBase	-	Cloud Base Height (lidar)
LowBaseT	-	Cloud Base Temperature (lidar)
LowRet	-	Cloud Base Height (radar)
LowRetT	-	Cloud Base Temperature (radar)
LW	-	Longwave Radiation
LWD	-	Longwave Radiation Down
LWU	-	Longwave Radiation Up
LWP	-	Column Integrated Liquid Water Path
MMCR	-	Millimeter Cloud Radar
MR	-	Surface Mixing Ratio
MWR	-	Microwave Radiometer
Net_CF	-	Net Cloud Forcing
RHI	-	Relative Humidity with Respect to Ice
RHW	-	Relative Humidity with Respect to Water
SD	-	Standard Deviation
SE	-	Standard Error

SHEBA		Surface Heat Budget of the Arctic Ocean
SHF	-	Surface Heat Flux
SW	-	Shortwave Radiation
SWD	-	Shortwave Radiation Down
SWU	-	Shortwave Radiation Up
SZA	-	Solar Zenith Angle
T1	-	Surface Temperature at 1 meter
T3	-	Surface Temperature at 4 meters
T5	-	Surface Temperature at 18 meters
TOA	-	Top-of-the-Atmosphere
Tsurf	-	Surface Temperature
TWP	-	Total Water Path
WDir	-	Surface Wind Direction at 4 meters
Wspd	-	Surface Wind Speed at 4 meters

ACKNOWLEDGMENTS

I would like to thank Dr. Matthew Shupe of the Cooperative Institute for Research in Environmental Science, University of Colorado, and the National Atmospheric Administration Environmental Technology Laboratory in Boulder, for generously providing the cloud dataset required for this study. Secondly, I would like to thank Prof. Peter Guest and Prof. Tom Murphree for their wisdom and guidance during the course of writing my thesis. Their patience and efforts in steering me in the right direction were greatly appreciated. Lastly, and most importantly, I would like to thank my wife, Kay, for her unwavering support (and for simply putting up with me).

THIS PAGE INTENTIONALLY LEFT BLANK

I. INTRODUCTON

A. BACKGROUND

Improving the understanding of the processes responsible for the dramatic decrease seen in recent decades in the areal coverage of Arctic sea ice has becomes one of the most important avenues of research in the geosciences. Since perennial sea ice is a primary indicator of Arctic climate change, a roughly 15% decrease in area since 1980 (Francis et al. 2005) with a negative monthly linear trend in overall sea ice extent from 1979 to 2006 (Serreze et al. 2007), is cause for concern. As discussed by Stroeve et al. (2007), even though the 13 models participating in the Intergovernmental Panel on Climate Change Fourth Assessment Report indicate declining Arctic ice cover during the 1953 to 2006 period, none capture the observed trend of -7.8% ($\pm$ 0.6%) per decade (approximately 100,000 km^2 per year) for the end of the summer melt season in September. Instead, the multi-model mean trend of -2.5% ($\pm$ 0.2%) is on average three times smaller, with none of the individual ensemble members having trends as large as those observed for this period. These results place the ensemble mean model forecasts approximately 30 years behind the current observed summer minima. The large scatter between individual model simulations, and between modeled and observed trends, introduces a great deal of uncertainty as to when a seasonally ice-free Arctic Ocean state could become a reality. As changes in Arctic climate will have far reaching, even global consequences, climate change presents significant national security challenges for the United States (CNA Corporation 2007).

Despite the climatic significance of the Arctic, many physical processes occurring in this region are still not well understood (Rinke et al. 2006). The ice loss itself is best viewed as a combination of natural variability in the coupled ice-ocean-atmosphere system and a growing radiative forcing that is associated with rising concentrations of greenhouse gases (Serreze et al. 2007). The loss of ice is a conflation of dynamic (e.g., changes in ice circulation in response to winds) and thermodynamic (e.g., changes in surface air and ocean temperatures) processes which govern the decline in sea ice extent.

For this study, we chose to investigate one of the key physical components of these processes; the radiatively important clouds. As discussed by Randall et al. (1998), studies have shown that different cloud parameterizations can cause large discrepancies in the simulations of Arctic climate. The dry atmosphere and high surface albedo amplify cloud radiative influences on the surface, making Arctic clouds particularly important over the Arctic Ocean, because they can significantly impact the melting, re-freezing, thickness, and distribution of the seasonal ice pack (Maykut and Untersteiner 1971; Intrieri et. al 2002b). Although extensive work has been done on understanding the effect of clouds on the Arctic surface, aspects of the ice-albedo and cloud-radiation-feedback mechanisms are still unknown as they appear to be a complicated function of cloud height, thickness, phase and particle size (Curry and Ebert 1992; Francis et al. 1999; Intrieri et al. 2002b). While modeling of Arctic cloudiness has made some progress, the large deficiencies that still exist in modeling the cloud-radiation relationship can only be improved by incorporating observational data into parameterization development (Shupe and Intrieri 2004). As many Arctic clouds are mixed-phase (Zuidema et al. 2005), better articulating the characteristics of Arctic mixed-phase clouds is vital to improving their modeled representation.

Using the annual cycle of cloud and radiation measurements made as part of the Surface Heat Budget of the Arctic Ocean (SHEBA) field program, we examined a 335-day time series consisting of 19 variables defining microphysical characteristics of ice, liquid, and mixed-phase clouds. Previously identified as being important in determining the properties of Arctic clouds involved in the surface radiation balance (e.g., Intrieri et al. 2002a, 2002b, Shupe and Intrieri 2004, Zuidema et al. 2005, Shupe et al. 2006), these measurements were combined with additional SHEBA surface measurements of nine other meteorological variables. Since many models parameterize liquid presence and amount as a function of temperature above a given threshold (Shupe and Intrieri 2004), with mixed-phase clouds posing the greatest challenge, the intent of this study is to offer a possible avenue of improvement to the parameterizations of Arctic clouds by incorporating other variables besides temperature.

B. SHEBA

On and around an icebreaking ship frozen into and drifting with the permanent ice pack in the Beaufort and Chukchi Seas north of Alaska, Ice Station SHEBA meandered from 75°N, 142°W to 80°N, 162°W over the course of a year between October 2, 1997, and October 11, 1998 (Perovich et al. 1999) (Figure 1). Using an extensive suite of state-of-the-art instruments, a major accomplishment of the SHEBA program was that for the first time, a wide range of Arctic ice, atmosphere, and ocean observations were made over a full annual cycle (Shupe and Intrieri 2004), resulting in a complete time series of parameters defining the state of the Arctic surface heat budget. Pertinent to this study are the measurements that were used to identify and quantify the properties of clouds that are important to the surface radiation balance. For a more thorough discussion of other aspects of the SHEBA experiment, refer to Perovich et al. (1999) and Uttal et al. (2002).

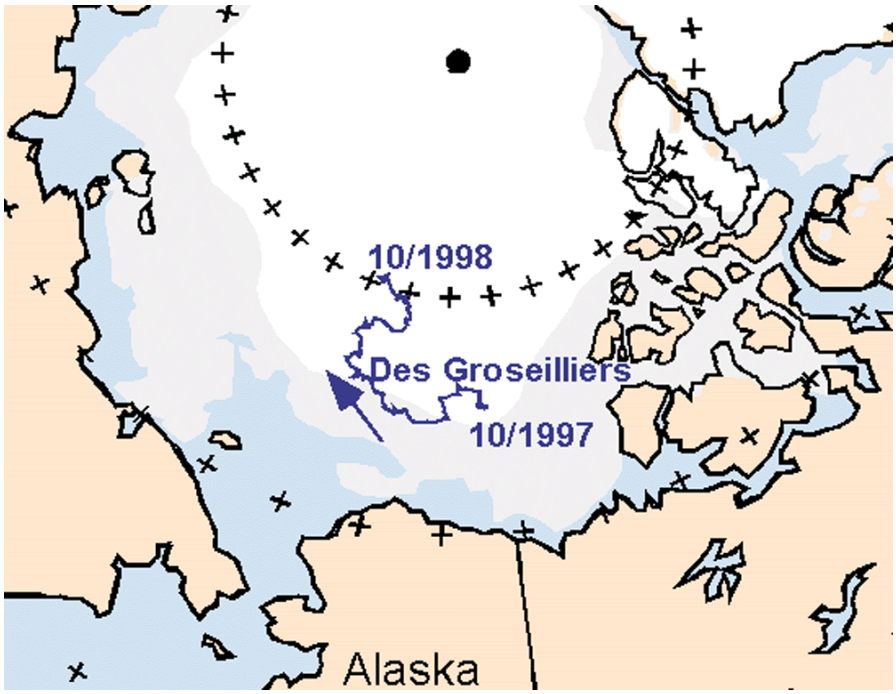

Figure 1. The year-long SHEBA drift. The blue line indicates the meandering path of the ice station from October 1997 to October 1998 [After Uttal et al. 2002].

1. Synoptic Considerations

When interpreting the results obtained from SHEBA, it must be kept in mind that the ice station was not stationary, but moved throughout the year with the ice in which it was anchored. The year-long field experiment traveled a distance of over 2,800 km, with a net displacement of 770 km. Daily drift distances ranged from as little as a few hundred meters to more than 30 km (Perovich et al. 1999). Therefore, any statistics are a function of both season and regional changes. For example, during the summer months, the ice station had drifted northwest and out of the Beaufort Gyre, directly exposing it to storms passing north through the Bering Strait. Therefore, the measurements during this time were heavily effected by significant synoptic activity. Furthermore, due to the influence of an El Nino at that time, there are indicators that the SHEBA year was particularly stormy (Intrieri et al. 2002b), especially in the winter, and therefore possibly cloudier than normal. Summer conditions were less stormy than usual (Guest, pers. comm.).

2. Surface-Based Instrumentation

In order to examine the characteristics of Arctic clouds that make them radiatively important to the surface, SHEBA was outfitted with a variety of ground-based remote sensors. These included broadband radiometers, a sun photometer, radiosondes, a microwave radiometer, and a lidar and radar. Specifications for these instruments are shown in Table 1. The instruments are summarized in more detail by Shupe et al. (2005), and additional information can be found in the provided references.

Additional surface-based measurements included in the cloud dataset used in this study (i.e., surface temperature and albedo) were recorded using instruments associated with the Atmospheric Surface Flux Group (ASFG) tower site at the SHEBA field station. As mentioned previously, this study also includes an additional dataset composed of near-surface measurements recorded during SHEBA, which were also made by instruments associated with the ASFG. A complete description of the ASFG and its instruments, including measurement uncertainties, can be found in Persson et al. (2002). Relevant to the final results of this study are the measurements of wind velocity, which

were measured by an AeroVironment Sodar (Model 4000) at a height of roughly 8 meters and a minimum stored resolution of the averaged data of 15 minutes. Sonic wind calibration uncertainties were sometimes large and unexplainable (Persson et al. 2002). The corrected wind speeds have standard deviation calibration errors of approximately 3% and twice that for the 95% confidence interval (Persson et al. 2002).

Surface-Based Instrumentation	Vertical Resolution	Application and Measurement Uncertainties
35-GHz Millimeter Cloud Radar (MMCR) $\lambda = 8.66mm$, K_a-band, (Moran et al. 1998)	Surface to 15 km above ground level (AGL) with 45 m range gate, average period of 9 seconds and 0.5^o beam width, and a sensitivity of -46 dBZ at 5 km without attenuation	Radar reflectivity profile, ice component retrieval (up to 73% uncertainty, Shupe et al. (2005)), Doppler spectrum (Intrieri et al. 2002b)
23.8- and 31.8-GHz Microwave Radiometer (MWR) (Westwater et al. 2001)	Integrated	Cloud column integrated liquid water path (LWP) Retrieval uncertainty 25 g m^{-2} (Shupe and Intrieri 2004)
$0.5235\mu m$ Depolarization and Backscatter Unattended Lidar (Alvarez et al. 1998)	Surface to 20km AGL with 30 m range resolution and time average of 5 seconds	Cloud phase, cloud base and top heights (Intrieri et al. 2002b)
GPS/LORAN atmospheric sounding radiosonde system	2 day^{-1} at 1200 and 2400 UTC.4 day^{-1} (addition of 0600 and 1800 UTC) during periods in April – July 1998	Standard atmospheric profiles Uncertainties for temperature 0.2^oC, and relative humidity 2-4% (Intrieri et al. 2002a)
Sun photometer (500 and $675nm$)	Integrated	Aerosol optical depth (tracks sun) (Zuidema et al. 2005)
Eppley Precision Infrared Radiometer hemispheric flux pyrgeometers		Longwave radiation Uncertainty for net surface fluxes $\pm$ 4 W m^{-2} (Persson et al. 2002)
Precision Solar Pyranometers		Shortwave radiation. Uncertainty for net surface fluxes 4.5% with negative bias of a few W m^{-2} (Persson et al. 2002)

Table 1. Surface-based instrumentation for measuring cloud characteristics; vertical resolution, application, measurement uncertainties and references.

C. CLOUD RADIATIVE FORCING

Cloud radiative forcing (CF) is defined as the radiative impact that clouds have on the atmosphere, surface, or top-of-the-atmosphere (TOA) relative to clear skies (Shupe and Intrieri 2004). Introduced by Ramanathan et al. (1989), the concept of CF was proposed as a means for understanding the types of roles that clouds play in climate change in terms of thermal or albedo effect. A study by Cess et al. (1990) revealed cloud feedback to be the major source of model differences in climate sensitivity and established cloud feedback as a major focus of research (Ramanathan and Inamdar 2006). Using both satellite and surface-based observations, CF has seen extensive application as an index of the importance of clouds in the global radiation balance, with surface-based methods providing a more direct and accurate, though limited sampling, of CF of the surface. It terms of the Arctic, characterizing cloud radiative effects is a critical component for understanding the current polar climate and an important step towards simulating potential climate change in polar regions (Intrieri et al. 2002a).

During SHEBA, cloud and surface-based radiation measurements were used to determine the impact that Arctic clouds have on the surface energy balance of sea ice over a complete annual cycle (e.g. Intrieri et al. 2002a, Shupe and Intrieri 2004, Zuidema et al. 2005). Previous surface CF estimates for the Arctic, such as studies by Curry and Ebert (1992) and Zhang et al. (1996), used climatological cloud properties and a 1-D radiative transfer model, respectively, to show that the average effect of polar clouds in comparison to clear skies is to warm the surface. The results of Zhang et al. (1996) also indicate that clouds not only warm the surface, but also warm the lower atmosphere, causing an earlier onset and faster rate of snowmelt. This warming effect is primarily a factor of the high surface albedo of ice and snow, and the lack of incoming solar radiation from the late fall to early spring, while surface cooling is experienced only during a few weeks in midsummer when clouds reflect a greater amount of insolation than the underlying surface would under clear sky conditions (Intrieri et al. 2002a). Satellite estimates of CF for the Arctic surface (Schweiger and Key 1994) also indicate similar results, with warming occurring for all months of the year except during June and July.

1. Cloud Forcing Definitions

For the purposes of this study, CF is defined as detailed in Intrieri et al. (2002a) and Shupe and Intrieri (2004), where the roles of cloud and environmental properties in Arctic surface CF are investigated using the observational dataset obtained from SHEBA.

Following Ramanathan et al. (1989), longwave (LW), shortwave (SW), and total CF parameters are given as

$$CF_{LW} = F(A_c) - F(0) \qquad (1a)$$

$$CF_{SW} = Q(A_c) - Q(0) \qquad (1b)$$

$$CF = CF_{LW} + CF_{SW} \qquad (1c)$$

Here, A_c is the cloud fraction, F and Q are the net surface LW and SW fluxes, respectively, and the first and second terms in (1a) and (1b) are all-sky and equivalent clear-sky conditions, respectively. All fluxes are defined as positive downwards. According to these definitions, the equivalent clear-sky terms are considered to be the net surface fluxes neglecting all direct cloud effects.

Defining CF in such a way provides a simple, yet very effective means of evaluating the impact of clouds on the surface energy balance by giving an indication of the effects that clouds have on the surface in comparison with clear skies (Intrieri et al. 2002a). If more radiation reaches the surface when clouds are overhead than when skies are clear, the clouds act to warm the surface (i.e., the thermal effect) and the CF value is positive. If less radiation reaches the surface when clouds are present than when skies are clear, the clouds act to cool the surface (i.e., the albedo effect) and the CF value is negative.

2. Surface Cloud Forcing During SHEBA

Surface CF was calculated on an hourly basis for the SHEBA year, using the definition of Ramanathan et al. (1989), as the measured net surface radiative flux minus the net flux had the skies been cloud free (Shupe and Intrieri 2004). Due to the high

frequency of clouds in the Arctic, rather than relying on sporadic measurements of clear sky conditions, clear sky LW and SW upwelling and downwelling surface radiative fluxes were calculated using a radiative transfer mode (the Santa Barbara Discrete Ordinate Radiative Transfer (DISORT) Atmospheric Radiative Transfer (SBDART) algorithm), the details of which are available in Intrieri et al. (2002a). Uncertainties in the CF calculations were due to model uncertainties, measurement errors, and instrument mismatches (Shupe and Intrieri 2004), with the measurement-based errors in CF_{LW} and CF_{SW} about 3 W m^{-2} and 4.5%, respectively. As the mean CF_{LW} under clear sky conditions was found to be 6.3 W m^{-2}, only forcing greater than this value are considered significant.

To investigate the roles of cloud and environmental properties in surface CF, Shupe and Intrieri (2004) expanded (1) using first-order atmospheric flux models. The resulting equations act as qualitative tools that are used to identify radiatively important properties, thereby providing a means for understanding and testing how changes in these properties affect the surface radiation balance. Using concurrent cloud property measurements from SHEBA, Shupe and Intrieri (2004) were able to further explore the CF data set as calculated and reported by Intrieri et al. (2002a) to reveal that cloud temperature and height, cloud microphysical composition, solar zenith angle (SZA), and surface albedo are the major components that contribute to surface CF (atmospheric transmittance also impacts CF, but was not examined in depth). Shupe and Intrieri (2004) also recognize cloud optical depth an important parameter as it influences both of the competing CF_{LW} and CF_{SW}, but instead use column-integrated liquid water path (LWP) as a surrogate for optical depth. As the SHEBA cloud dataset used in this study is derived from the dataset used by past analyses (e.g., Shupe and Intrieri 2004), we also use LWP in place of cloud optical depth.

The surface CF results, though not meant to be taken as representative for the entire Arctic region, nor be representative for all years, were felt by the authors to be a reasonable description of how clouds influence the surface radiative balance of the permanent ice pack of the Arctic Ocean (Shupe and Intrieri 2004). Major conclusions that directly relate to this study include (Intrieri et al. 2002a; Shupe and Intrieri 2004):

1. Over the course of the annual cycle, the net effect of Arctic clouds is to warm the surface, with a slight cooling effect over a short period during summer when surface albedo is low and clouds reduce the downwelling solar flux. Liquid clouds are significant in the overall positive surface CF in that they act as insulating layers, as well as being predominately responsible for the negative surface CF during the summer.

2. Surface CF is a complex function of cloud phase, optical depth, LWP, particle size, emitting temperature, height, SZA and surface albedo. Cloud phase alone does not directly control CF_{LW}, but plays an important indirect role in defining microphysical composition. However, cloud phase does have a direct influence on CF_{SW} due to the differences in scattering properties between spherical water droplets and non-spherical ice crystals.

3. The sensitivity of CF_{LW} to cloud fraction is approximately linear, and increasing sensitivity to cloud presence as cloud fraction increases. When LW effects are stronger (most of the year), an increase in cloudiness will cause greater surface warming relative to current conditions. The positive correlations is known as the cloud greenhouse effect, and is particularly important in the Arctic due to the absence of solar energy for much of the year and because prevalent, low-level cloud layers often reside within strong temperature inversions (Shupe and Intrieri 2004). On the other hand, the sensitivity of CF_{SW} is dependent on the total insolation. Surface cooling is enhanced with increased cloud cover when SW shading effects are stronger (midsummer). This negative correlation is the cloud albedo effect.

4. Best estimates for the annual average surface CF are -9 W m^{-2} in the SW and 38 W m^{-2} in the LW. Total CF is roughly 30 W m^{-2} for the fall, winter, and spring, falling to a minimum of -4 W m^{-2} in early July.

5. Liquid-containing clouds dominate Arctic surface CF. Annual mean CF_{LW} values are 52, 16, and 6 W m^{-2} for liquid-containing clouds, all-ice clouds, and clear skies, respectively. Regardless of season, all-ice clouds never contribute

more than 10 W m^{-2} to the mean surface CF. The Annual mean CF_{SW} values are -21 W m^{-2} and -3 W m^{-2} for liquid-containing and all-ice clouds, respectively. During the high insolation summer months, liquid-containing clouds can cool the surface by as much as 100 W m^{-2}, indicating that liquid-containing clouds have a higher albedo (i.e., higher optical depth and lower transmittance) than all-ice clouds.

6. Of the LW radiatively important cloud scenes observed, 95% had bases below 4.3 km. During winter, spring and summer, 95% of the radiatively important cloud scenes had base temperatures warmer than -36^{o}, -30^{o}, and -10^{o}C, respectively. The largest CF_{LW} values are mostly from clouds that are warmer than -15^{o}C, while clouds colder than -30^{o}C are usually indistinguishable from clear skies. Clouds with temperatures in between these values have a range of CF_{LW} from close to 0 W m^{-2}, to over 60 W m^{-2}.

7. Arctic LW radiative balance is strongly affected by frequent temperature inversions. Low-level liquid-containing clouds dominate the radiative balance, while ice clouds are not as important. Clouds with the largest positive CF_{LW} had bases less than 0.5 km. Though CF_{LW} decreases with height, this is primarily a function of cloud temperature in that CF_{LW} actually increases with cloud height for a constant cloud temperature. Therefore, as cloud temperature increases, CF_{LW} increases.

8. CF_{LW} is very sensitive to LWP for LWP < 30 g m^{-2}, but insensitive to higher LWPs, at which point clouds act as blackbody emitters. Therefore, changes in LWP are most important in high, optically thin yet relatively warm clouds, such as the frequent Arctic winter mixed-phase clouds that reside within a strong temperature inversion (Shupe and Intrieri 2004).

9. CF_{SW} is also sensitive to LWP. As LWP increases, so does CF_{SW} but the cloud SW shading effect continues to increase after the LW greenhouse effect is saturated.

10. CF_{SW} is limited by the TOA insolation, and therefore undergoes an annually averaged diurnal cycle, with no cycle in winter to maximum monthly averaged amplitude of 60 W m^{-2} in midsummer.

11. SW shading effects are strongest when the sun is highest in the sky. At the highest observed sun angles, average cooling for liquid containing and all-ice clouds was -15 and -55 W m^{-2}, respectively.

12. Cloud induced SW surface cooling increases with decreasing surface albedo. As albedo decreases, CF_{SW} cooling effect increases as relatively more SW radiation is absorbed by the surface under clear skies, with the sensitivity of CF_{SW} increasing from winter to summer. A decrease in surface albedo will cool the surface in the SW, resulting in a negative radiation feedback.

The observation-based data set on surface CF obtained from SHEBA provides baseline measurements that allow for the extrapolation and experimentation of different cloud scenarios (e.g., increasing or decreasing cloud amount or percentage of clouds containing liquid) in order to understand how evolving cloud conditions may affect sea ice (Intrieri et al 2002a). Even though a comprehensive cloud-radiation feedback assessment remains a difficult challenge, this type of data is being used to gauge the performance of models (e.g., Inoue et al. 2006, Rinke et al. 2006) in capturing the correct shape and sign of seasonal trends (Intrieri et al. 2002a). As discussed in Zuidema et al. (2005), the SHEBA CF and cloud property data can be used to investigate plausible climate change scenarios and their impacts on the net CF of the Arctic surface, examples of which include recent Arctic observations that indicate an increase in spring and summer cloudiness and a decrease in winter cloudiness (e.g., Wang and Key 2003), and dramatic surface reflectance changes such as the current decrease in Arctic sea ice. Specifying cloud parameters correctly in models will be one critical factor for assessing cloud impact in the Arctic (Intrieri et al 2002a), with the important aspect of cloud-phase being the focus of this particular study. Furthermore, given that this study also involved the separation of "liquid-containing" clouds into liquid-phase and mixed-phase clouds, general characteristics of liquid-phase and mixed-phase CF as measured during the SHEBA annual cycle are documented in the "Results" section.

D. GENERAL CHARACTERISTICS OF LIQUID-CONTAINING AND ALL-ICE CLOUDS OBSERVED DURING SHEBA

During SHEBA, Arctic cloud occurrence, base and top echo boundary heights, number of layers, and phase information, were well documented over the course of the annual cycle by combining the detection strengths of cloud radar and depolarization lidar. The collocated measurements provided a comprehensive, time-height view of cloudiness on an hourly time scale, where a cloud was considered to be present if either instrument observed a hydrometeor return (Shupe and Intrieri 2004). Due to the fundamental physical differences between transmitting at optical and millimeter wavelengths, substantial differences sometimes occurred between the echo boundaries detected by the lidar and radar. As discussed by Intrieri et al. (2002b), analytically integrating lidar and radar provides the most accurate cloud boundary measurements. For the cloud statistics presented here, echo base height, top height, and layer number were determined individually by lidar and radar to separate cloudy from cloud-free regions. These data were then combined to produce the cloud statistics. If the lidar was working, its base heights were used; otherwise, the radar heights were used. For cloud tops, the highest measured echo from either instrument was used. Between the two instruments, there was essentially 100% data coverage during SHEBA, implying that the monthly fraction of cloud occurrence is quite accurate (Intrieri et al. 2002b). Presented here are the general statistics of the key aspects of clouds observed during SHEBA. For complete details on both the instruments used and on the annual cycle of Arctic cloud characteristics, please refer to Intrieri et al. (2002b).

1. Cloud Occurrence

The resulting cloud morphology data set from SHEBA (Intrieri et al. 2002b) revealed that within the sampled region, the Arctic was cloudy about 85% of the year, with the least amount of cloudiness during the winter (~70%) and maximum cloud occurrence during the summer (~90%), indicating that clouds were almost continuously present. Monthly averaging of cloud occurrence identified a maximum of 97% during September and a minimum of 63% during February. Existing climatological data sets

derived from satellite and surface-based observations (e.g., Key et al. 1999, Vowinkel and Orvig, 1970, Warren et al. 1988), though not relying on the same parameter (cloud fraction vs. cloud occurrence as presented here), generally indicate less cloud cover, ranging from 80% in summer to 40-60% in winter (Intrieri et al. 2002b). Possibilities for why these numbers are lower than those indicated by SHEBA include lower detection rates in winter by surface observers, identification problems over ice/snow associated with satellite techniques, different locations, and as previously mentioned, the possibility of a cloudier SHEBA year during the winter and less cloudy during the summer.

2. Cloud Bases, Heights, and Layers

Monthly averages of cloud base and top heights displayed no distinct seasonal trend, with bases varying between 0.25 and 1.6 km above ground level (AGL) and top heights ranging between 2.8 and 5.5 km AGL. Though most months exhibited a significant distribution of low cloud bases above 1 km in the atmosphere (January, May, June, August and September being the exceptions), the highest frequency of occurrence of the lowest cloud bases was in the lowest 1 km for all months, indicating the presence of boundary layer clouds throughout the year. This statistic is particularly noteworthy given that the lowest cloud bases should be the most significant in effecting surface radiative fluxes (Intrieri et al. 2002b). Corresponding cloud top heights were more evenly distributed between 0 and 10 km AGL, with all months except for September having a bimodal distribution indicating the presence of surface boundary layer clouds (tops 0.5 to 1 km AGL) and mid- and upper-level clouds (tops 6 to 8 km AGL). The number of well defined (and often thin) stratus layers was typically one or two, with two or more occurring more often in the spring and summer. June and July exhibited the highest incident of four or more layers, while single layers were more prevalent during the rest of the year (except for November, when the occurrence of single and multiple layers was approximately equal).

3. Liquid or Ice

Correctly characterizing cloud phase is one of the most critical requirements for determining the radiative impact of clouds on the surface (Sun and Shine, 1994; Intrieri et al. 2002b). Lidar measurements of depolarization ratios (less than 0.11 indicate liquid, greater than 0.11 indicate ice) revealed that clouds containing liquid water existed throughout the entire annual cycle at SHEBA; the percentage of lidar-observed clouds containing liquid was 73% for the year (Intrieri et al. 2002b). The greatest occurrence of clouds with liquid water was during the summer (95%, June to August), with the most detected in July (95%), while spring saw a large fraction of clouds with liquid as well (73%, March to May). Surprisingly, liquid-containing clouds occurred with a relatively high and previously unexpected frequency during winter (45%, November to February), with the smallest monthly average occurring in December (23%). Generally, clouds containing liquid were concentrated within the lowest 1 km of the atmosphere, especially during the spring and summer months, but were frequently observed up to 4.5 km AGL, and occasionally up to 6.5 km AGL. Ice-phase clouds, on the other hand, were evenly distributed between the surface and 10 km AGL, and occurred 38% of the time that clouds were observed during SHEBA (Shupe et al. 2005) with no obvious annual trend. In comparison, all-liquid cloud layers were observed 19% of the time that clouds were observed during SHEBA (Shupe et al. 2005). Following the annual cycles of atmospheric temperature and moisture, most all-liquid clouds occurred during May through September, and the least during December through April.

LWP was derived from brightness temperatures measured by a microwave radiometer (MWR), with a retrieval uncertainty of 25 g m^{-2} (Westwater et al. 2001; Shupe and Intrieri 2004). Even though both the lidar and MWR were used to provide independent measurements of whether or not liquid exists in the vertical column, the limitations of each instrument preclude the ability to fully characterize the phase of all clouds observed during SHEBA (Shupe and Intrieri 2004). For the MWR, LWP values greater than the retrieval uncertainty indicate the presence of liquid but without a vertical location, while the lidar depolarization ratio can indicate liquid at a vertical location, but the signal attenuates in optically thick clouds, preventing measurements of higher cloud

layers. During SHEBA, the lidar detected liquid 72% of the time that clouds were present, and 49% of all time, while the MWR indicated 50% and 41%, respectively (Shupe and Intrieri 2004). Therefore, since these two techniques for identifying liquid in the column do not always agree, the atmosphere is considered to contain cloud liquid in some amount if either instrument detects liquid. All-liquid cloud annual mean LWP was found to be roughly 45 g m^{-2}, while the annual mean all-ice cloud ice water path (IWP) was measured to be 30 g m^{-2} (Shupe et al. 2005). Though not explicitly discussed in this study, liquid water content retrieval uncertainties ranged between 49% and 72%, while ice water content uncertainty was 62% to 100% (Shupe et al. 2005).

4. Cloud Temperatures

The last important general characteristic of Arctic clouds observed during SHEBA is the relationship between cloud type and cloud temperature as measured by radiosondes, with temperature profiles linearly interpolated to the millimeter cloud radar's time-height grid (Shupe et al. 2005). Liquid-containing clouds occurred at surprisingly cold temperatures and over a wide range with a seasonal variation. For example, during January, liquid-containing clouds existed at temperatures between -34^o to -13^{o}C, while in July they occurred between -30^o and +10^{o}C. All ice clouds were present over an even wider temperature range that also varied seasonally and with a mean temperature of -31^{o}C. In December, ice clouds were observed between -60^{o}C and -15^{o}C, while during July they occurred between -50^o and 0^{o}C. At no time was liquid recorded below -40^{o}C, while only liquid existed above 0^{o}C (Shupe et. el. 2005).

E. ARCTIC MIXED-PHASE CLOUD UNCERTAINTIES

Mixed-phase clouds are an understudied component of global cloudiness and are thus poorly represented in models at all scales (e.g. Gregory and Morris 1996, Morrison et al. 2003, Shupe et al 2006). Due to the unique radiative properties of liquid droplets and ice particles, the proper partitioning of cloud phase is particularly important, but has proved to be very challenging. Model parameterization schemes typically partition cloud phase as a function of temperature; however, the appropriate temperature range over

which multiple phases can coexist is in question (Shupe et al. 2006). Even though observations, including those conducted at SHEBA (e.g. Intrieri et al 2002b), have shown that liquid water can exist at temperatures as low as -30^{o} to -40^{o}C, the range of the lower temperature limit parameterized in models can be anywhere from -40^{o}, -23^{o},-15^{o}, to -9^{o}C (Shupe et al 2006). The uncertainties in mixed-phase parameterization have not only been shown to have a strong impact on the ability to simulate the present-day climate (Gregory and Morris 1996) and play crucial roles in climate prediction modeling (Sun and Shine 1995), but model studies indicate that the impacts of different mixed-phase parameterizations are more pronounced at higher latitudes (Sun and Shine 1995). The limited set of observations and studies concerning mixed-phase clouds leaves substantial ambiguity in our understanding of these clouds, their properties, and their important mechanisms (Shupe et al. 2006). Such voids in knowledge concerning mixed-phase clouds are particularly true for the Arctic, where mixed-phase clouds are common, challenging to characterize, and important to the radiative forcing of the ice-covered surface (Zuidema et al. 2005). Therefore, data collected from field programs such as SHEBA provide vital information that can be used to address these deficiencies and provide possible improvements to cloud parameterization schemes, which is the focus of this study.

1. Arctic Mixed-Phase Clouds Observed During SHEBA

Clouds observed above the SHEBA ice camp were classified as being all ice, all liquid, mixed-phase, or precipitating (Shupe et al. 2006) according to measurements made by the ground-based instruments previously discussed and by surface observer logs. An in-depth discussion outlining the operational cloud property and classification retrieval suite can be found in Shupe et al. (2005). Using the data obtained from SHEBA, studies have been conducted that improve our understanding of Arctic mixed-phase clouds in terms of their basic statistics, microphysical properties, and cloud-radiation-surface-feedbacks (e.g. Zuidema et al. 2005, Shupe et al. 2006). Although methods do not currently exist to operationally retrieve all microphysical properties of mixed-phase clouds (Shupe et al. 2006), significant and useful information can be derived from the

SHEBA measurements that can elucidate the need for improving their parameterization in models at all scales. As general characteristics of liquid-containing and all-ice clouds have been previously discussed, what follows is a more detailed description concerning important properties of mixed-phase clouds observed during SHEBA, with an emphasis on those characteristics pertinent to this study. When appropriate, comparisons are made with liquid-phase and ice-phase clouds as documented in Shupe et al (2005). The range of mixed-phase cloud macrophysical properties observed during SHEBA is consistent with other reported studies, while variations among microphysical properties can be large. However, the in situ observations suggest that the average mixed-phase microphysical properties derived from the SHEBA measurements are within a reasonable range of past in situ observations (Shupe et al. 2006). The information presented here is not intended to be a thorough description of mixed-phase cloud microphysics. For a summary of the current understanding of mixed-phase cloud properties and processes, as well as a more detailed account of aspects pertaining to the mixed-phase clouds observed at SHEBA, please refer to Shupe et al. (2006).

a. Definition of a Mixed-Phase Cloud

Mixed-phase clouds are defined loosely as clouds that have liquid and ice coexisting near each other, usually within the same vertical column (Zuidema et al. 2005). Generally, the clouds classified as mixed-phase during SHEBA were of a stratiform nature, and are the most prominent and documented type in the Arctic. As discussed by Shupe et al. (2006), stratiform mixed-phase clouds are frequently topped by a thin layer of cloud liquid that produces small ice particles that quickly grow and precipitate from the base of the liquid layer, and many mixed-phase clouds also contain embedded regions of liquid. The definition of mixed-phase clouds used here does not imply that all portions of clouds classified as mixed-phase contain both ice and liquid in the same volume (Shupe et al. 2006). Furthermore, the mixed-phase profile statistics as presented in the following sections are for cloud layers that were well developed, contained only one distinct layer, and had tops limited to 5 km AGL. The particulars of thicker, multilayered mixed-phase clouds are not discussed given their complex nature.

b. Mixed-Phase Cloud Occurrence, Height, Thickness, Temperature, and Cloud Surface Forcing

Over the course of the SHEBA annual cycle, mixed-phase clouds occurred 41% of the time, and 59% of the time that clouds were present (Shupe et al. 2005; Shupe et al. 2006). Of the mixed-phase clouds observed, over half were low-level, single-layer stratiform clouds. Monthly mixed-phase cloud fraction ranged from a minimum of 10% in December, to a maximum of 70% in September, with more mixed-phase clouds occurring during the spring and fall transition seasons. The transition seasons also exhibit the lowest mixed-phase cloud bases, with an average height of 0.5 km AGL, though over half of the observed bases were at the lowest radar range gate. During the summer months, the average mixed-phase cloud base increased to 1-3 km AGL, while the winter's average base was 1 km AGL. Cloud thickness also followed a seasonal trend, being moderately thinner in May and thicker in midsummer than during other times of the year, with an average of roughly 1-3 km with bases near the surface.

A somewhat perplexing feature of Arctic mixed-phase clouds is that, via the Bergeron process, they might be expected to glaciate rather rapidly, but they in fact tend to be rather long-lived (Verlinde et al. 2007). On average, the mixed-phase clouds observed during SHEBA persisted for 12-hours, with many mixed-phase cloud systems persisting for multiple days with only minor intermediate breaks in mixed-phase cloudiness (Shupe et al. 2006). The most persistent mixed-phase cloud lasted for 6.4 days, while one large-scale springtime mixed-phase boundary layer system investigated by Zuidema et al. (2005) lasted for nearly 10 days.

Mixed-phase cloud temperatures derived at each radar range gate within the cloud layers varied on a seasonal basis, with a monthly average of -25^{o}C in December to a maximum above -10^{o}C in June. During the spring transition season, cloud temperatures ranged between -25^{o} and -10^{o}C, while fall mixed-phase cloud temperatures were between -20^{o} and -5^{o}C. In general, observed mixed-phase clouds temperatures ranged between -40^{o} and 0^{o}C, with most observations between -25^{o} and -5^{o}C. The few occurrences of mixed-phase cloud temperatures above 0^{o}C (0.3%) were due to particles falling from mixed-phase layers that encountered warmer temperatures at lower altitudes

(Shupe et al. 2006). For mixed-phase and liquid-phase clouds composed of only a single layer below 5 km, average cloud temperatures were roughly -17.5^{o} and -11.5^{o}C for mixed-phase and liquid-phase clouds, respectively.

In an investigation of a particularly long-lived spring-time boundary layer mixed-phase cloud system that occurred during SHEBA, Zuidema et al. (2005) revealed that the radiative impact of mixed-phase clouds on the Arctic surface can be significant. Due to the persistent cloud presence (roughly 10 days), the downwelling SW fluxes were significantly reduced, with a time-mean decrease of 55 W m^{-2} relative to clear sky conditions. However, due to the high surface albedo during this time (0.85), the CF_{SW} averaged only -12 W m^{-2}. In contrast, even though downwelling LW fluxes only increased by 49 W m^{-2} compared to clear skies, the average mean CF_{LW} was 53 W m^{-2}. This resulted in a time-mean net CF of 41 W m^{-2} modulated by a diurnal amplitude of roughly 20 W m^{-2}. The net CF value is significant given that 40 W m^{-2} is capable of warming 1 m of ice by 1.8 K day^{-1}, neglecting heat transport (Zuidema et al. 2005). Though cloud optical depth was not directly considered for this study, an important finding by Zuidema et al. (2005) was that for low-optical-depth cloud columns, such as boundary-layer mixed-phase clouds, CF is very sensitive to changes in cloud optical depth, while high-optical-depth cloud columns were sensitive to changes in surface albedo. This has significant implications for future climate change scenarios, in that the net CF of the Arctic surface might be most affected by changes in surface reflectance, such as the decrease in sea ice extent and thickness.

The characteristics of mixed-phase CF as measured during the SHEBA annual cycle are documented in the "Results" section of this study.

c. Mixed-Phase Cloud Liquid and Ice

In general, the mixed-phase clouds observed during SHEBA contained more liquid and ice than single-phase clouds (Shupe et al. 2006). The annual mean ice water path (IWP) was 42 g m^{-2}, which is 40% larger than that of observed ice-phase clouds. Similarly, mixed-phase LWP derived from MWR measurements (single-layer clouds) tended to be slightly larger than that of observed liquid-phase clouds. The annual

mean LWP was 61 g m^{-2}, which is 30% larger than that of observed liquid-phase clouds. For mixed-phase and liquid-phase clouds composed of only a single layer below 5 km, annual mean LWPs were 43 and 23 g m^{-2}, respectively.

The amount of liquid relative to ice in mixed-phase clouds generally increases with cloud top temperature (Shupe et al. 2006). On average, liquid-dominant mixed-phase clouds had cloud top temperatures in the range of -25° to 0°C, while ice-dominant mixed-phase cloud top temperatures ranged between -35°C to -10°C. At temperatures between -40° and -30°C, 87% of mixed-phase clouds had liquid fractions, defined as LWP divided by the total water path (TWP), or (LWP+IWP), of 0 to 0.25, with few occurrences of higher values. As temperatures increase, the probabilities of higher liquid fractions increase due predominately to increases in LWP with temperature (i.e., as explained by the Clausius-Clapeyron equation), rather than due to a decrease in IWP. The annual average relationship between temperature and liquid fraction indicate a transition from full glaciation at -24°C to complete liquid water at -14°C, with some indication of a temperature relationship that varied moderately with season. However, at any given liquid fraction, temperatures varied over approximately 20° to 25°C (Shupe et al. 2006).

F. SUMMARY OF ARCTIC CLOUD PARAMETERIZATION

Temperature plays a key role in determining mixed-phase cloud occurrence and composition, and the fact that they tend to occur during the transition seasons suggests that the temperature range during those times of the year is most conducive for the coexistence of multiple cloud phases (Shupe et al. 2006). Of particular importance to climate model parameterization is the relationship between mixed-phase cloud temperature and liquid fraction. Even though observations support phase partitioning with temperature, the spread of available observations is large, indicating that differences in temperature-phase relationships should be expected as conditions impacting this relationship differ regionally and possibly seasonally based on available moisture sources, ice-forming nucleus type and concentration, vertical motion, and net cooling rate (Shupe et al. 2006). As discussed by Shupe et al. (2006), the measurements made by

SHEBA and similar Arctic cloud observation programs indicate that liquid water occurs at temperatures much colder than some model parameterization allow, supporting parameterization schemes that can have cloud liquid as low as -40^{o}C. Furthermore, that a range of roughly 25^{o}C exists at any given liquid fraction with a phase transition relationship that may vary with season complicates the ability to accurately parameterize the partitioning of cloud phases based solely on temperature. None of the parameters (cloud height and thickness, total LWP or IWP) investigated by Shupe et al. (2006) could completely explain the observed spread in the phase transition relationship. As such, Shupe et al (2006) concluded that cloud phase parameterization based on additional parameters will likely be necessary in order to capture Arctic cloud phase variability and distributions.

G. MOTIVATION FOR THIS STUDY

This study is motivated primarily by unresolved issues concerning model parameterizations of Arctic cloud phase:

1. Clouds are a fundamental component of the Arctic surface energy balance. They are particularly important over the Arctic Ocean, as clouds can significantly impact the melting, re-freezing, thickness, and distribution of the seasonal ice pack. However, aspects of the impact of clouds on the surface, and indeed many features of the clouds themselves, are still unknown and/or difficult to characterize, introducing a great deal of uncertainty into modeled representations of Arctic clouds.

2. Studies have shown that different cloud parameterization schemes can produce large variations in the simulations of Arctic climate. The large scatter between individual model results, and between modeled and observed trends, further complicates the assessment of current Arctic climate change. As changes in Arctic climate are likely to have global consequences, climate change presents significant national security concerns for the United States.

3. The correct characterization of Arctic cloud phase is one of the most critical requirements for determining the radiative impact of clouds on the surface,

with liquid-containing clouds identified as dominating the CF of the Arctic surface. However, this has proved to be particularly challenging, given that liquid water can exist to temperatures as low as -40^{o}C, which is much colder than most model parameterizations allow.

4. Of particular importance to model parameterization is the relationship between mixed-phase cloud temperature and liquid fraction. Even though observations support cloud phase partitioning with temperature, the spread of available observations is large. Furthermore, a range of roughly 25^{o}C exists at any given liquid fraction, complicating the ability to accurately parameterize the partitioning of cloud phases based solely on temperature.

5. Past studies have concluded that a broader analysis of Arctic cloud and environmental features is necessary to further constrain the cloud phase-temperature relationship in order to improve model phase partitioning parameterizations.

Given these unresolved issues, our primary goal with this study is to examine the annual cycle of SHEBA measurements for liquid, ice, and mixed-phase Arctic clouds, combined with additional coincident surface observations, and develop a possible method for improving phase-partitioning using other readily available observed parameters besides temperature.

In the following chapter, our data and analysis methods are presented. Chapter III presents our main results. Chapter IV provides the summary of our results, discussion and conclusion, and suggestions for possible future research.

THIS PAGE INTENTIONALLY LEFT BLANK

II. DATA AND ANALYSIS METHODS

A. SHEBA CLOUD-PHASE DATASET

Dr. Matthew D. Shupe from the Cooperative Institute for Research in Environmental Science, University of Colorado, and the National Atmospheric Administration Environmental Technology Laboratory in Boulder, provided the SHEBA cloud dataset required for this study. This dataset is essentially the same dataset that was used to derive the Arctic cloud properties previously discussed; however, there are important differences. In order to fit the needs of this study, Dr. Shupe partitioned the cloud dataset in a way that was different from that used in past analyses. For example, when liquid-containing clouds were identified, this was based on information obtained from the measurements of LWP from the MWR and the lidar depolarization ratio. If either instrument identified liquid, then that time step was included in the liquid-containing cloud scenes. A new data field for cloud type was also created specifically for this study that did not exist in past analyses. Furthermore, Dr. Shupe set criteria for identifying reasonable data and for eliminating outliers that would have otherwise skewed important statistics.

The differences in dataset partitioning between that used in this study and in the previous SHEBA cloud studies explored in the "Background" section produced small discrepancies in dataset statistics. However, the differences are small enough to be considered insignificant, and can certainly be accounted for and attributed to the uncertainties of the methods (Shupe, pers. comm.).

1. SHEBA Cloud Dataset Description

The dataset used for this study consists of a 335-day time series beginning on 01 November 1997 and ending on 01 October 1998 using the Julian decimal day format. There are 19 variables defining observed and derived microphysical and radiation characteristics for seven types of cloud scenes (Table 2).

Cloud Dataset Variables
LowRet (km) (Cloud Base; Height of lowest hydrometeor return typically from radar)
LowRetT (°C) (Temperature of LowRet cloud base)
LowBase (km) (Cloud Base; Same as LowRet but with additional lidar information)
LowBaseT (°C) (Temperature of LowBase cloud base)
Tsurf (°C) (Surface Temperature)
LWP (g m^{-2}) (Liquid Water Path)
IWP (g m^{-2}) (Ice Water Path)
LWD (W m^{-2}) (Longwave Radiation Flux Down)
LWU (W m^{-2}) (Longwave Radiation Flux Up)
CF_LWD (W m^{-2}) (Longwave Cloud Forcing Down)
CF_LWU (W m^{-2}) (Longwave Cloud Forcing Up)
CF_LW (W m^{-2}) (Longwave Cloud Forcing)
SWD (W m^{-2}) (Shortwave Radiation Flux Down)
SWU (W m^{-2}) (Shortwave Radiation Flux Up)
CF_SWD (W m^{-2}) (Shortwave Cloud Forcing Down)
CF_SWU (W m^{-2}) (Shortwave Cloud Forcing Up)
CF_SW (W m^{-2}) (Shortwave Cloud Forcing)
Albedo
SZA (degrees) (Solar Zenith Angle)

Table 2. SHEBA cloud dataset variables with abbreviations and units.

All data are 1-hourly averages. LWP measurements were not available prior to 05 December 1997 due to instrument calibration problems. Neither LowRet nor LowBase are always an accurate specification of cloud base height (Shupe, pers. comm.). For this study, LowBase was chosen as the variable for defining cloud base height as lidars have a more accurate measurement of cloud base (Intrieri et al. 2002b).

The seven cloud types (Table 3) that compose this dataset contain both multiple- and single-layer clouds. It would be fairly difficult to separate multi- and single-layer clouds, given that the observations are difficult to interpret and there are a number of different ways to define "single-layer" (Shupe, pers. comm.). There are certainly complex multi-layered scenes included in the mixed-phase category, but such cases appeared to be infrequent (Shupe, pers. comm.). As multi-layered mixed-phase cloud scenes often occurred with another cloud type, the majority were placed in the "More than One Phase" category. Therefore, the mixed-phase clouds as classified in this study can be considered to be predominantly single-layer clouds. During times when there was 0.5-hour of a liquid-phase cloud, followed by 0.5-hour of an ice-phase cloud, the complete 1-hour period is classified as "More than One Phase". For this particular study, only liquid-phase, ice-phase, and mixed-phase clouds are investigated.

None
Only Liquid-Phase
Only Ice-Phase
Only Mixed-Phase
Rain + Cloud
Snow + Cloud
Drizzle + Cloud
More than One Phase

Table 3. Cloud Types.

2. SHEBA Surface Dataset Description

The surface dataset was obtained from Dr. Peter Guest of the Naval Postgraduate School and consists of a subset of nine surface variables defining meteorological parameters that were measured during SHEBA at the ASFG tower site. All data were quality controlled and verified by members of the ASFG and Environmental Technology Laboratory. Given that this dataset uses the same Julian decimal day format, it was merged with the cloud dataset so that all measurements from both datasets are coincident with each other. Therefore, it covers the exact same time period and consists of 1-hour averages for each variable. The surface variables used in this study are listed in Table 4.

Surface Meteorological Dataset Variables
Wspd (m s^{-1}) (Surface Wind Speed at 4 meters)
WDir (degrees) (Surface Wind Direction at 4 meters)
T5 (^{o}C) (Surface Temperature at 18 meters)
T3 (°C) (Surface Temperature at 4 meters)
T1 (°C) (Surface Temperature at 1 meter)
MR (g kg^{-1}) (Mixing Ratio at 4 m)
RHW (%) (Relative Humidity with respect to Water at 4 m)
RHI (%) (Relative Humidity with respect to Ice at 4 m)
SHF (W m^{-2}) (Sensible Heat Flux at 4 m)

Table 4. SHEBA surface meteorological dataset variables with abbreviations and units. Heights were nominal.

B. ANALYSIS METHODS

Five Matlab programs were used to convert the cloud dataset text file into a useable database. The first program inputs the cloud dataset text file, removes the extraneous text, assigns variable names, and fills the resulting database with usable data. A second program takes the newly created database and performs basic statistical calculations on each variable for a given cloud type. In order to produce visual representations of the dataset, a subset of five programs creates time series plots for each cloud phase that depict annual trends, variable relationships, and aid in identifying any correlations. The fourth and fifth programs were used to merge the surface meteorological dataset with the cloud dataset, calculate the liquid fractions of the three cloud phases, perform and plot bin averaged statistics, derive a best fit to the liquid fraction data, and calculate multi-variable regression statistics.

1. Basic Statistic Calculations

Basic statistical calculations allowed for direct numerical comparisons of each of the 19 variables associated with each cloud phase. The statistical calculations include total number of data points, number of good data points, percentage of bad data, mean and median, standard deviation (SD), and minimum and maximum values.

SD was calculated in Matlab using the following equation, where "N" is the number of samples taken, and "$\bar{X}$" is the mean of a discrete uniform random variable "X";

$$SD = \sqrt{\frac{1}{N}\sum_{i=1}^{N}(X_i - \bar{X})^2}$$

In terms of basic statistics, SD was used in describing the overall distribution of a particular variable. During the portion of this study concerned with improving phase-partitioning parameterization, a similar equation was used in order to evaluate the ability of the fits to capture the data. Instead of using the overall mean, the fitted (predicted) data was used. In this way, SD can be viewed as the "random error", which gives the estimate of the error of any single prediction when using the fit of the data. Of course,

the error is not really random since it actually depends on complicated physical processes and the distribution lacks a typical bell shape. However, it is a useful way to describe the expected accuracy of the fit of liquid fraction data.

Although it is more applicable to truly random events, standard error (SE) was calculated in Matlab using the following equation, where "n" is the number of good values;

$$SE = \frac{SD}{\sqrt{n-1}}$$

For the liquid fraction data fit, SE estimates the confidence in the mean values, and can be considered the estimate of the accuracy of the derived fit to the data. In other words, the true fit might be different, given that it takes into account all possible natural conditions, rather than a data sample, which was the case with this study.

A final statistical calculation that was performed was to determine the percent variability (variance) that was captured by the fit of the liquid fraction data. This was defined as;

$$\%Variability = 100 - 100\left(\frac{VarianceOfError}{VarianceOfLiquidFraction}\right)$$

2. Multi-variable Regression

In addition to approximately 100 time series plots, we also performed 90 multi-variable regressions, or fitted lines using bin average statistics as guides, using the variables available from both datasets. As detailed further in the "Results" section of this study, best fits were attempted using built-in Matlab curve fitting functions, but due to artifacts of the data sampling, these produced results that were not representative of the data statistics.

III. ANALYSIS AND RESULTS

A. CLOUD PHASE STATISTICS

The cloud dataset used for this study contains a total of 8,040 hourly observations covering 335 days. Each observation is composed of a cloud type with measurements of 19 variables defining the average characteristics of that cloud type over the course of that 1-hour period. A total of 2,941 of these observations were of liquid, ice, or single-layer mixed-phase clouds. Relative to each other, liquid, ice, and mixed-phase clouds occurred 17.6%, 39.4%, and 42.9% of the time, respectively. These results support previous observations documenting the predominance of mixed-phase clouds in the Arctic. In regards to the full dataset of seven different cloud scenes (including clear sky), liquid, ice, and mixed-phase clouds were recorded 6.44%, 14.4%, and 15.7% of the time, respectively. Therefore, the three cloud scenes chosen for this study represent only a fraction of the total types of cloud conditions (including precipitating) that existed during the annual cycle.

Previous CF studies using SHEBA cloud observations, such as those discussed in the "Background" section, did not separate liquid and mixed-phase clouds, but instead combined them as "liquid-containing" clouds when performing their statistical analyses. As a result, an analysis of their individual CF characteristics could not be accomplished. The main reason for not separating the two cloud phases is that liquid is the dominant phase in terms of the surface radiation balance. Since both types of clouds contain liquid, the difference between liquid and mixed-phase clouds is thought to be small and insignificant. As such, the radiatively important difference between single and mixed-phase cloud scenes is considered to be that between ice-phase and mixed-phase clouds. Given that this study uses a SHEBA cloud observation dataset that separates liquid-phase and mixed-phase clouds, it provides an opportunity to investigate each cloud type's CF.

Although statistical calculations were carried out on all 19 cloud variables, these parameters have been examined by previous studies as detailed in the "Background" section. They were performed during this study as a means of quality control; a way of

comparing our results with those of other published studies. Only CF statistics and the statistics pertaining to variables that directly impact this study are discussed.

1. Liquid-Phase Clouds

Presented in Table 5 are the basic statistical calculations for liquid-phase clouds as observed during the SHEBA annual cycle. Total CF is calculated as;

Net_CF = CF_LW + CF_SW

Variable	Mean	Minimum	Maximum
LowBase (km)	0.34334	0.09	4.582
LowBaseT (^{o}C)	-10.376	-33.36	7.259
LWP (g m^{-2})	27.716	-17.319	312.23
CF_LW (W m^{-2})	38.05	-15.99	79.899
CF_SW (W m^{-2})	-14.958	-134.64	15.561
Net_CF (W m^{-2})	23.146	-84.579	72.532

Table 5. Liquid-phase cloud statistics: mean, minimum, and maximum values.

Most liquid-phase cloud base heights averaged below 0.5 km AGL, indicating the presence of boundary layer clouds throughout the year (Figure 2). Minimum liquid-phase cloud temperatures indicate that all liquid clouds existed at temperatures as cold as the -30^{o}C's, and averaged roughly -10^{o}C (Figure 3). Liquid-phase LWPs averaged approximately 28 g m^{-2}, but were as high as 312 g m^{-2} (Figure 4). The negative LWP in the minimum statistic is an artifact of the retrieval algorithm.

The strong surface cooling effect that liquid-phase clouds can have is reflected in the strongly negative CF_SW minimum value of -135 W m^{-2}, which is highly dependent on solar insolation and surface albedo (Figures 5a-b). The positive mean liquid-phase Net_CF of 23 W m^{-2} indicates that the over all effect of liquid-clouds is to warm the surface over the course of the year (Figure 6). This surface warming effect of liquid-phase clouds can be very strong, as indicated by the maximum Net_CF value of roughly 73 W m^{-2}. The minimum Net_CF value of -84 W m^{-2} illustrates the cloud albedo effect as experienced during the summer months, where the net effect of optically opaque liquid-phase clouds is to cool the surface.

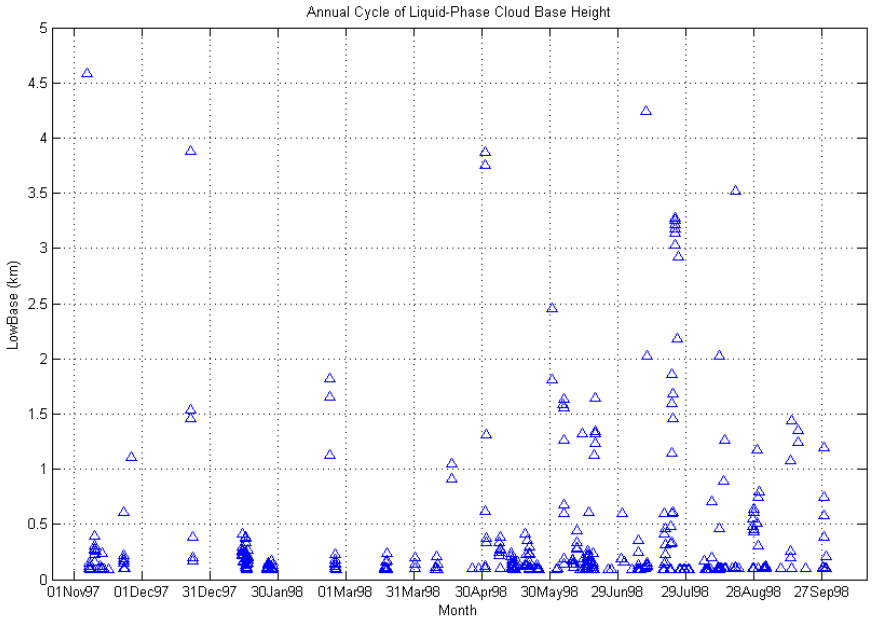

Figure 2. Annual cycle of liquid-phase cloud base height. The time range (x-scale) is from 01 November 1997 to 01 October 1998, and is marked in 30-day increments. The majority of liquid-phase clouds exist below 0.5 km AGL for the majority of the year, indicating the dominance of radiatively important boundary layer clouds. The increase in liquid-phase cloud base heights in late spring through the fall reflects the occurrence of warmer temperatures during those seasons.

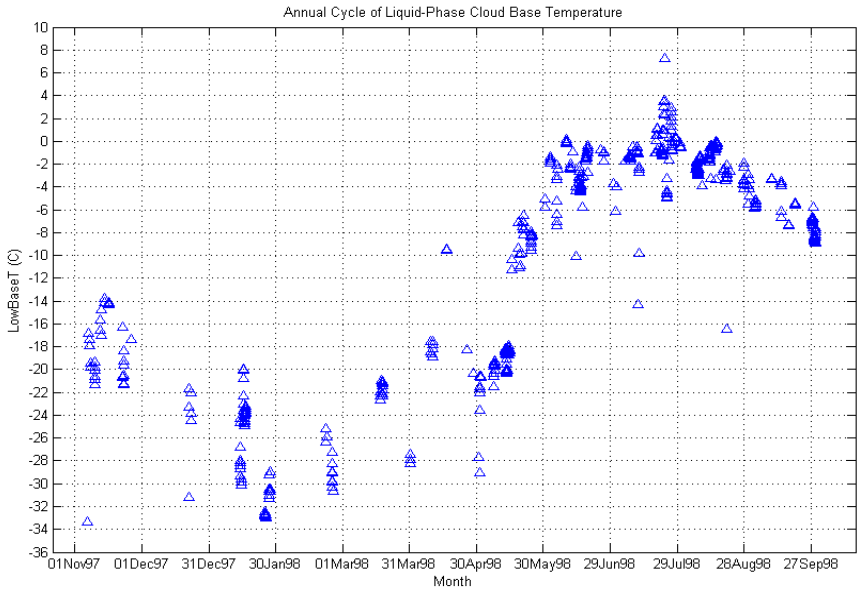

Figure 3. Annual cycle of liquid-phase cloud base temperature. Cloud base temperatures follow a seasonal trend, where the coldest recorded temperatures occur during mid-winter, while the warmest temperatures follow in late summer.

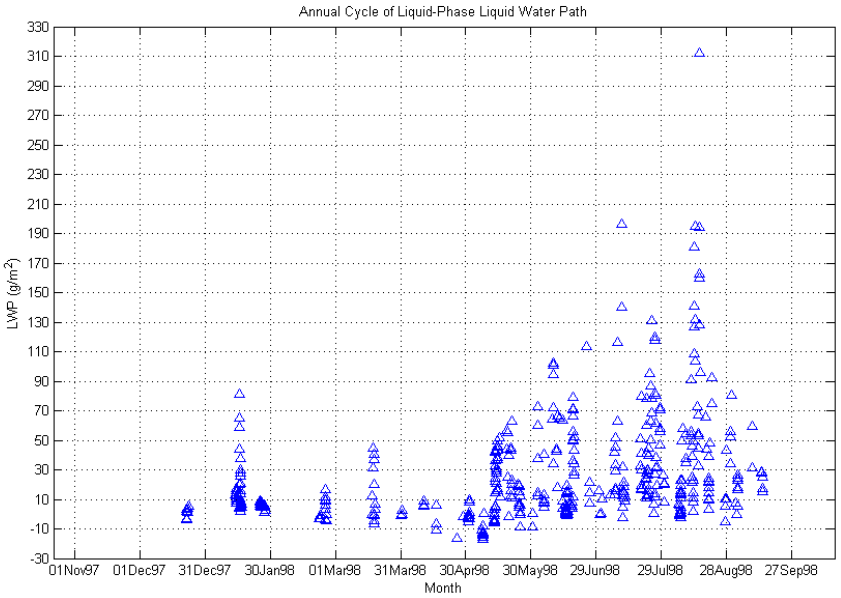

Figure 4. Annual cycle of liquid-phase cloud LWP. LWP increases with the warmer summer temperatures. As LWP increases, clouds become optically thicker and transmittance decreases, resulting in strong SW surface cooling in the summer.

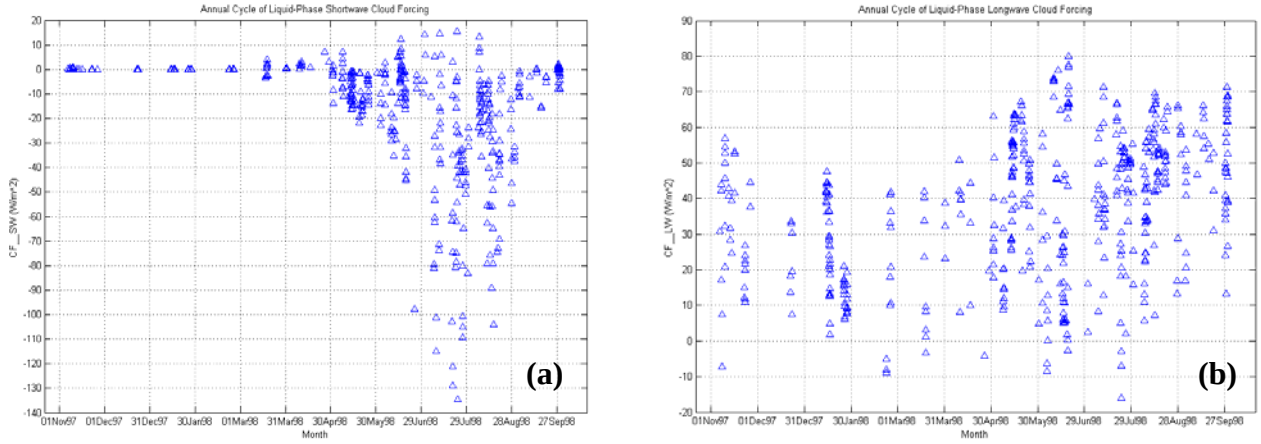

Figure 5. Annual cycle of liquid-phase CF_SW and CF_LW. CF_SW (a) is strongly negative during the summer months, which results in a negative overall Net_CF during that time. CF_LW (b) is predominately positive during the entire year, with larger values occurring during spring through fall, as the clouds are warmer than during the winter months.

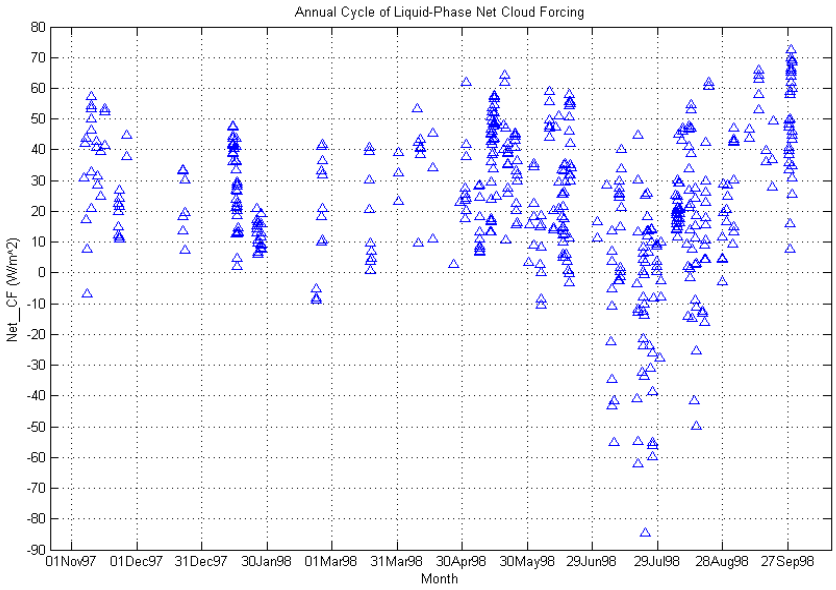

Figure 6. Annual cycle of liquid-phase Net_CF. Net_CF is generally positive during winter, and negative during a few weeks in the summer. Liquid-clouds have a strong warming effect in winter. During the summer, however, their high albedo (large LWP) results in strong surface cooling.

2. Ice-Phase Clouds

Presented in Table 6 are the basic statistic calculations for ice-phase clouds as observed during the SHEBA annual cycle.

Variable	Mean	Minimum	Maximum
LowBase (km)	2.8712	0.09	9.622
LowBaseT (^{o}C)	-27.723	-61.449	3.092
IWP (g m^{-2})	27.384	0.003	946.78
CF_LW (W m^{-2})	17.572	-22.62	71.239
CF_SW (W m^{-2})	-1.5679	-116.91	28.301
Net_CF (W m^{-2})	15.983	-51.864	71.239

Table 6. Ice-phase cloud statistics: mean, minimum, and maximum values.

As cloud base heights averaged roughly 3 km AGL, the majority of ice clouds occurred above the boundary layer (Figure 7). Maximum cloud base heights near 10 km AGL were the highest recorded out of the three cloud phases and represent cirrus clouds. Any ice-phase cloud temperatures over 0^{o}C should be considered suspect. The mean cloud base temperature was roughly -28^{o}C, but temperatures as low as -61^{o}C were recorded (Figure 8). Ice-phase IWPs were on average 27 g m^{-2}, but were recorded as high as 947 g m^{-2} (Figure 9). Ice-phase mean Net_CF of approximately 16 W m^{-2} again shows how clouds, even those composed entirely of ice, have a net warming effect on the Arctic surface (Figures 10a-c).

A notable result of the statistics for ice-phase IWP and liquid-phase LWP is that on average, both types of clouds contain nearly the same amount of water. Even with the same water content, ice-phase mean Net_CF is much smaller than that of liquid-phase clouds, indicating the much greater effect liquid clouds have on the Arctic surface.

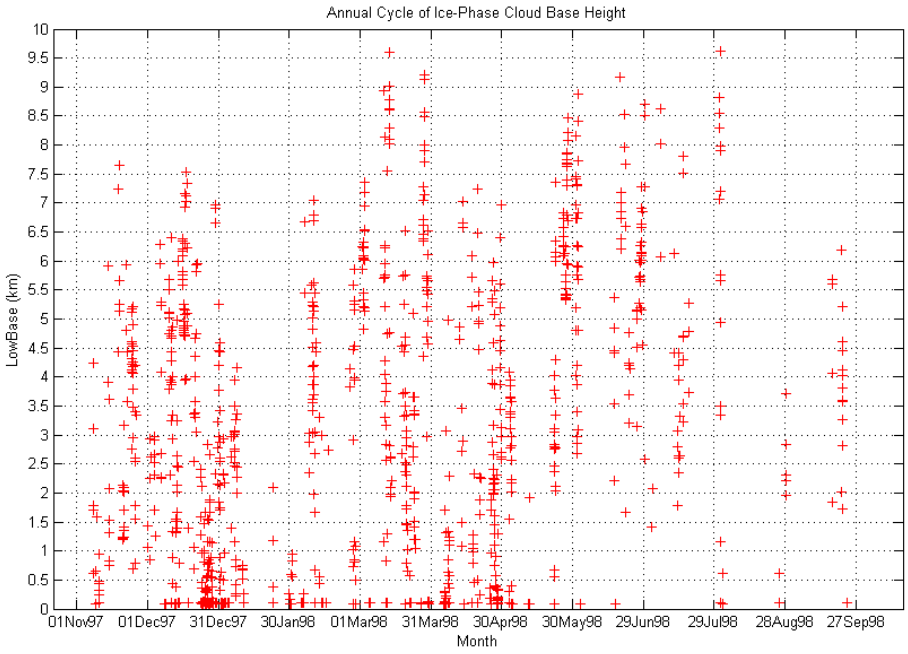

Figure 7. Annual cycle of ice-phase cloud base height and temperature. The majority of ice-phase cloud base heights (a) are above 1 km AGL, indicating how most occur above the boundary-later. During the warmer summer and fall months, the frequency of ice-phase clouds decreases, especially in the lower levels.

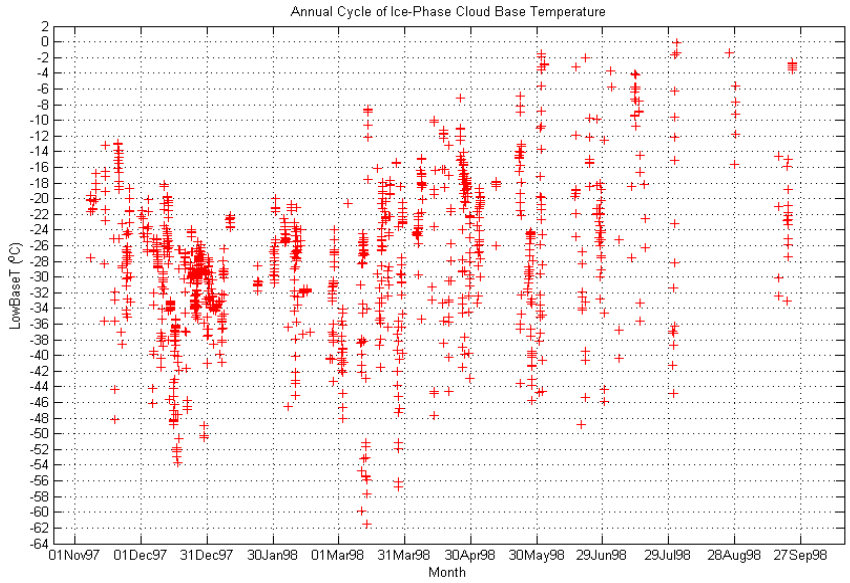

Figure 8. Annual cycle of ice-phase cloud base temperature. Cloud base temperatures generally follow a seasonal trend, being colder in the winter and warmer in the summer.

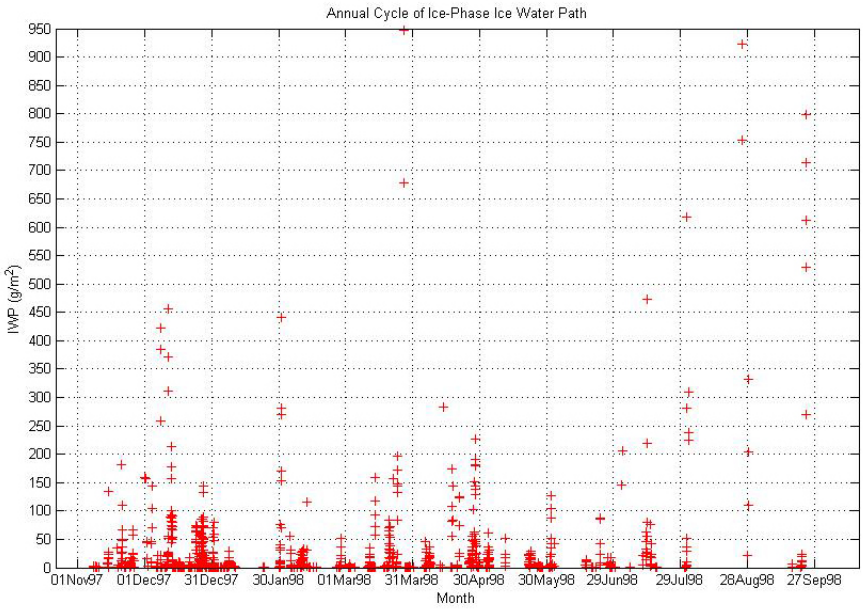

Figure 9. Annual cycle of ice-phase IWP. Most IWPs are below 10 g m^{-2}, with larger values indicating the existence of optically thicker ice-clouds.

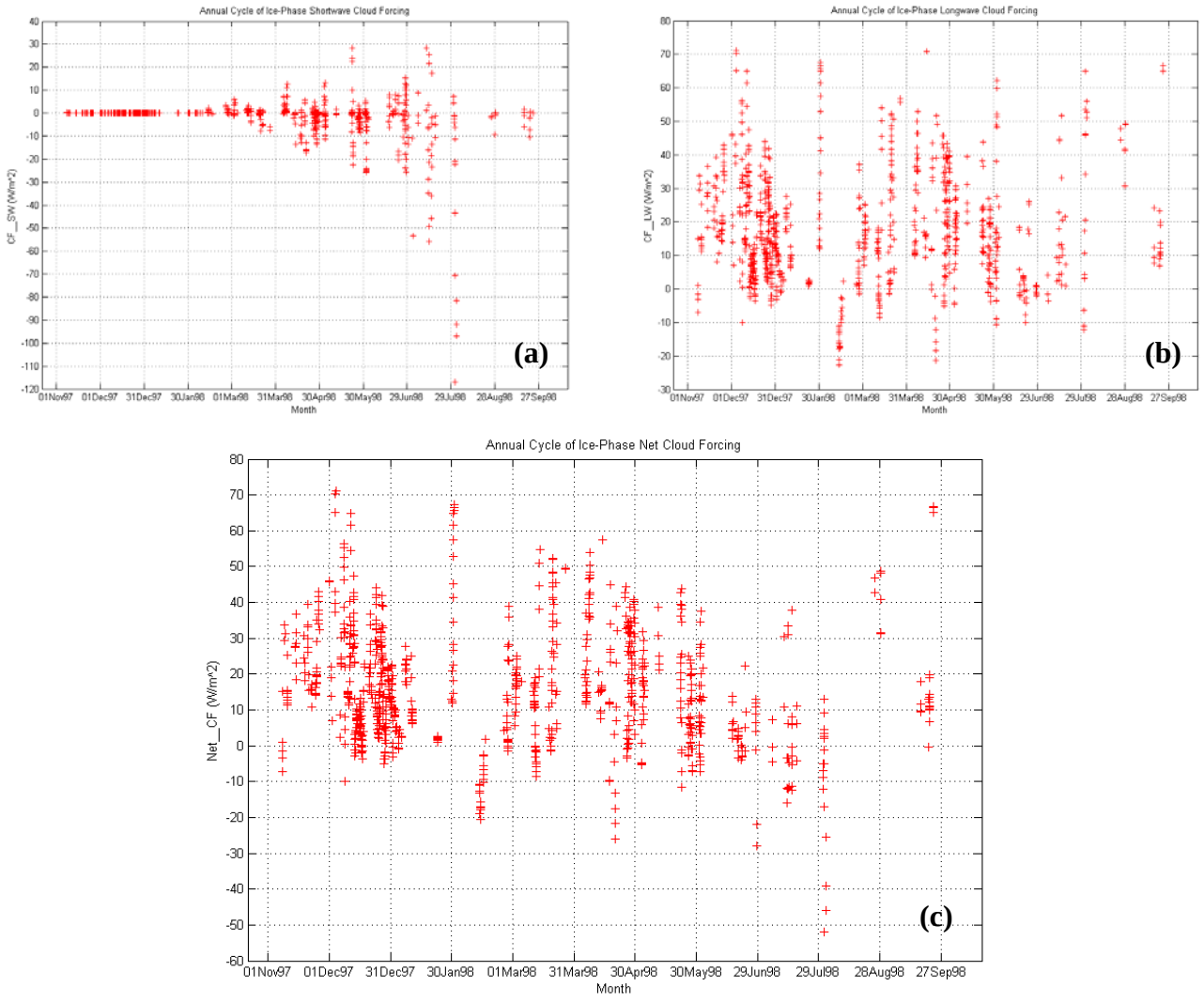

Figure 10. Annual cycle of ice-phase Net_CF, CF_SW, and CF_LW. Although smaller in magnitude than liquid-phase clouds, the plot of CF_SW (a) indicates that the SW shading effect can be strong enough to induce cooling of the surface, especially during the summer. The occurrence of large positive CF_LW (b) values during winter and spring indicate how some ice-phase clouds are optically thick enough (Figure 9) to induce a warming of the surface. The annual cycle of Net_CF (c) indicates that even ice clouds have a net warming effect on the Arctic surface for the majority of the year.

3. Mixed-Phase Clouds

Presented in Table 7 are the basic statistical calculations for mixed-phase clouds as observed during the SHEBA annual cycle.

Variable	Mean	Minimum	Maximum
LowBase (km)	0.59463	0.09	5.177
LowBaseT (^{o}C)	-14.302	-39.719	0.422
LWP (g m^{-2})	40.847	-19.002	271.13
IWP (g m^{-2})	31.905	0.003	766.03
CF_LW (W m^{-2})	49.237	-18.24	81.62
CF_SW (W m^{-2})	-7.3397	-116.54	34.342
Net_CF (W m^{-2})	42.004	-59.813	80.379

Table 7. Mixed-phase cloud statistics: mean, minimum, and maximum values.

As with liquid-phase clouds, average mixed-phase base heights were confined to the lower 1 km of the atmosphere, indicating the dominance of boundary layer clouds (Figure 11a). Mean mixed-phase cloud base temperature was roughly -14^{o}C, but temperatures as low as -40^{o}C were recorded, indicating the presence of liquid water at surprisingly cold temperatures (Figure 11b). Mean LWPs and IWPs averaged 41 g m^{-2} and 32 g m $^{-2}$, respectively, which are both higher than liquid-phase LWP and ice-phase IWP, indicating that mixed-phase clouds contain, on average, more liquid and more ice than single-phase clouds (Figures 12a-b). Mean Net_CF for mixed-phase of 42 W m $^{-2}$

was nearly double that of liquid-phase mean Net_CF, which illustrates the greater average annual surface warming effect that mixed-phase clouds have over liquid-phase clouds (Figures 13a-c). These results clearly indicate how mixed-phase clouds are the most important contributor to the Arctic surface radiation balance, and therefore stress the need for improving model phase-partitioning parameterization (Figure 15).

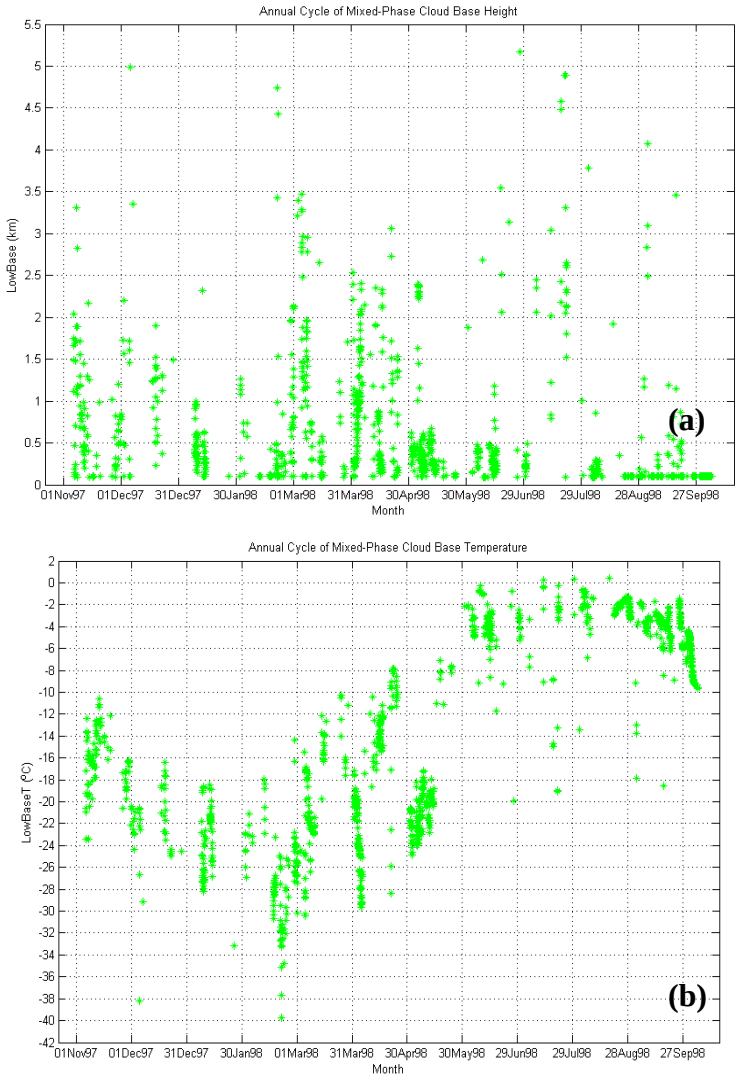

Figure 11. Annual cycle of mixed-phase cloud base height and temperature. The majority of mixed-phase cloud base heights (a) are below 1 km AGL, indicating that most were radiatively important boundary layer clouds. Cloud base temperature (b) follows a seasonal trend, with the coldest temperature in the winter, and warmest in the height of the summer. As indicated by the plot, liquid water can occur at surprisingly cold temperatures.

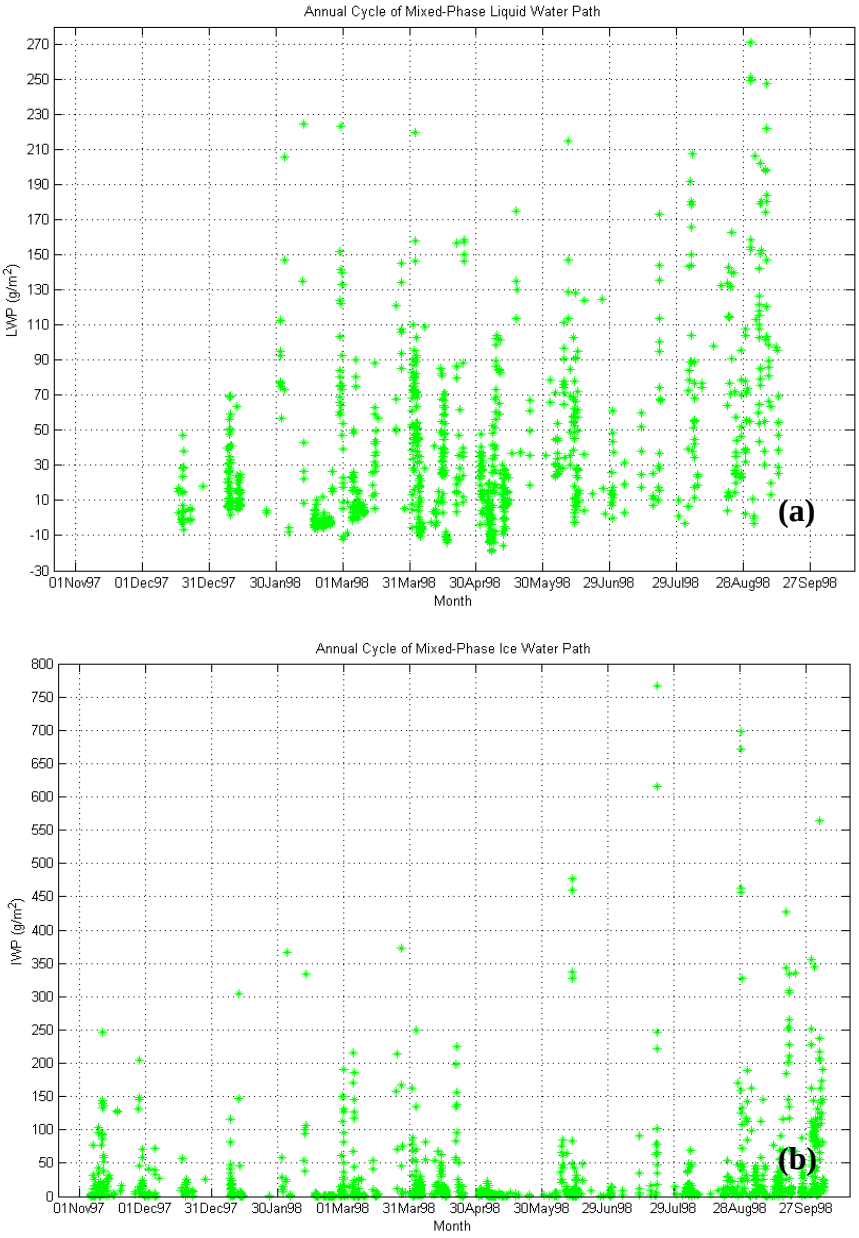

Figure 12. Annual cycle of mixed-phase LWP and IWP. Overall amounts of both LWPs (a) and IWPs (b) are larger than single phase clouds, which are directly related to the larger CF effects that mixed-phase clouds have on the Arctic surface. The plot of LWP (a) shows how many mixed-phase clouds are below the blackbody threshold of LWP = 30 g m^{-2}, especially during the spring transition season, indicating that small changes in their LWPs will lead to large changes in their LW effects on the surface. LWP amounts increase and larger amounts are more common in the summer due to warmer temperatures.

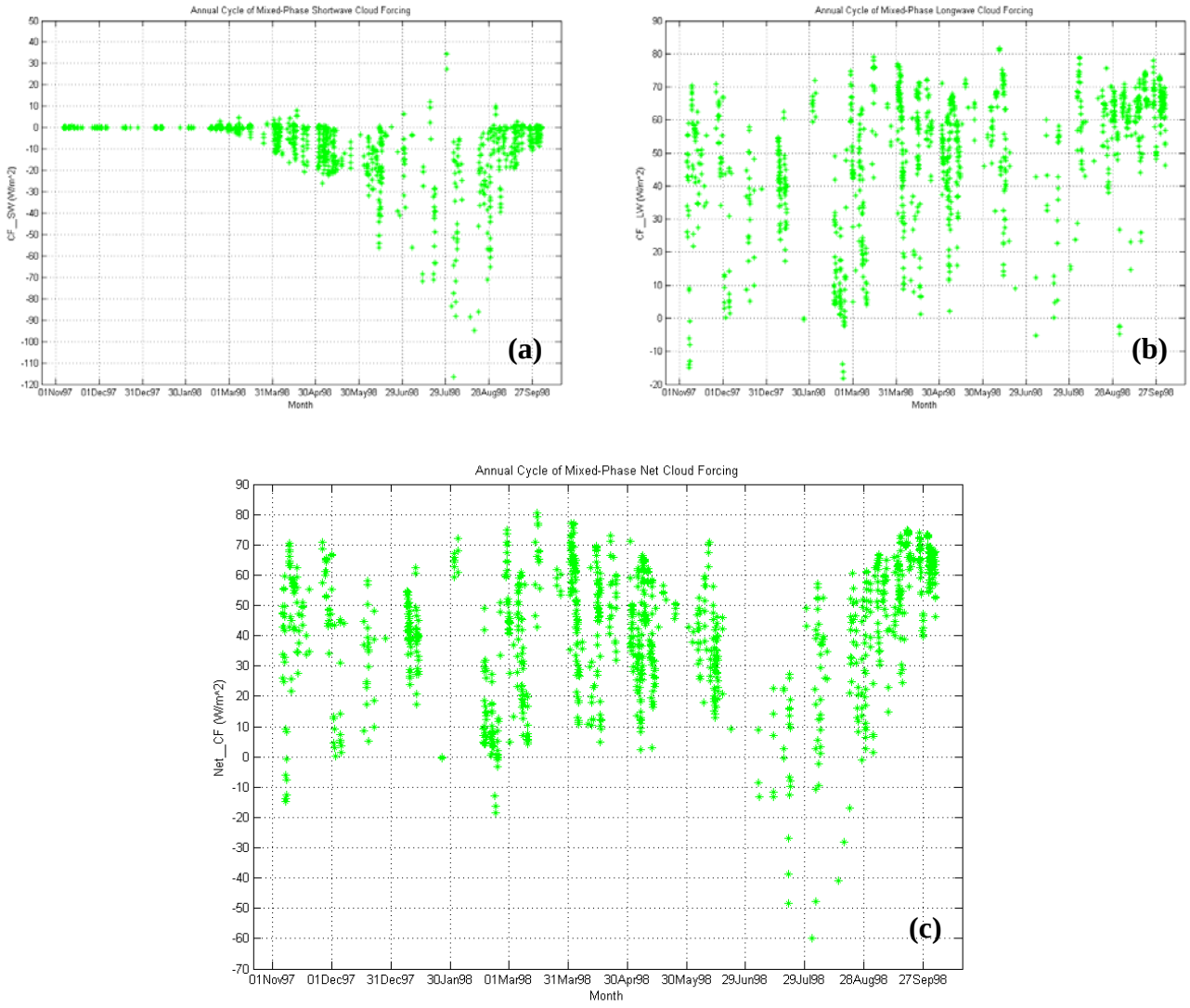

Figure 13. Annual cycle of mixed-phase Net_CF, CF_SW, and CF_LW. CF_SW (a) has a strongly negative component in the spring through the fall, having a maximum cooling effect August. The sharp decrease in CF_SW in the fall has to do with decreasing sun angles. CF_LW (b) is generally all positive, with an increasing positive trend from winter to fall, possibly due to warming temperatures and larger LWPs. Net_CF (c) is generally positive during the winter and negative during the summer, indicating how clouds warm the surface in winter, but cool it for a few weeks in the summer when sun angles are high and surface albedo is low. Overall Net_CF trend is generally larger in the positive than single-phase clouds.

4. Liquid and Ice Water Paths

As previously discussed, liquid is the dominant phase in terms of the radiation balance of the Arctic surface, particularly in the LW. To explore the differences in CF between liquid clouds and ice clouds, plots of "liquid-containing" clouds and ice-phase clouds were created in relation to their resulting CF_LW (Figures 14a-b) and CF_SW (Figures 15a-b). The scatter in data points is probably due to variations in cloud temperature and height, as well as variation in hydrometeor size. As noted by previous studies (e.g., Shupe and Intrieri 2004), the different CF response between all ice and liquid-containing clouds is probably due to the relatively few large ice crystals that generally compose ice-phase clouds, as opposed to many small liquid droplets that make up "liquid-containing" clouds. Ice clouds have less surface area per unit volume, giving them much less optical depth and a higher transmittance than liquid-containing clouds. These results further emphasize the need to correctly represent Arctic "liquid-containing" clouds in model parameterization, as well as shed light on some of the differences in CF, as represented in previous figures in this study.

Though not explicitly depicted in Figure 14, for liquid-containing clouds at typical Arctic cloud temperatures, CF_LW increases until LWP = 30 g m^{-2}, after which point clouds emit as blackbodies. This is a LW saturation effect that has been noted often in the literature (Shupe and Intrieri 2004). However, the bin average curves that we constructed for the plots clearly indicate that the sensitivity of LW and SW to LWP and IWP is greatest at smaller values. Therefore, as previously noted in this study and discussed by Shupe and Intrieri (2004), changes in LWP are more important in high, optically thin, yet relatively warm clouds, such as the frequent winter mixed-phase clouds that reside within often occurring strong temperature inversions. Unfortunately, due to the retrieval uncertainty of the MWR, adequate measurements of LWP in the high-sensitivity regime below 25 g m^{-2} are inadequate (Shupe and Intrieri 2004).

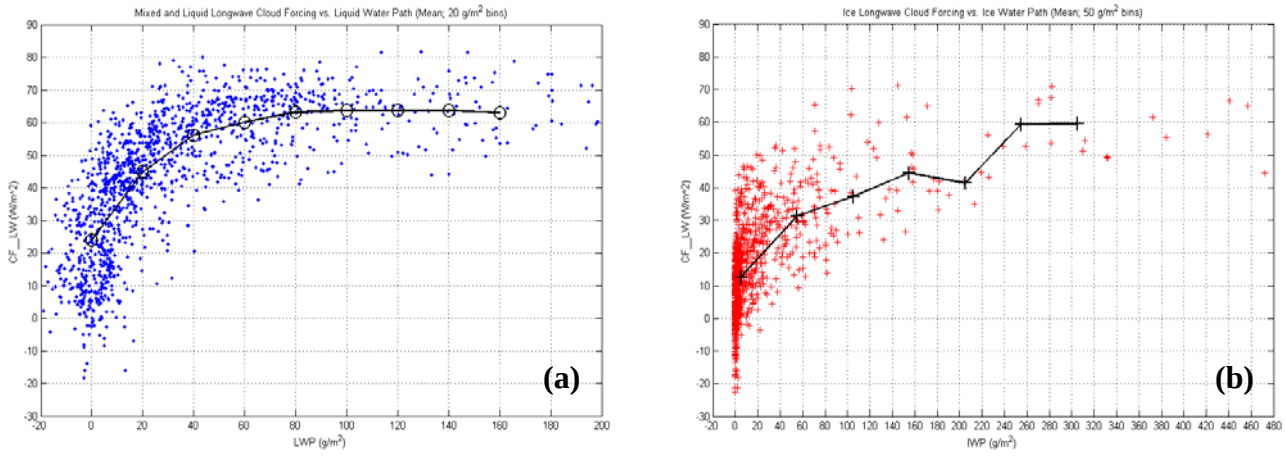

Figure 14. CF_LW for "liquid-containing" and ice-phase clouds in relation to LWP and IWP. Liquid and mixed-phase clouds were combined together as "liquid-containing" clouds (a) in order to emphasis the radiative importance of accurately predicting Arctic cloud liquid content. In comparison with ice-phase clouds (b), for given LWP or IWP, the CF_LW effects are stronger for liquid. The bin average curves in each plot also represent how the sensitivity in the LW to LWP and IWP is greatest at smaller values.

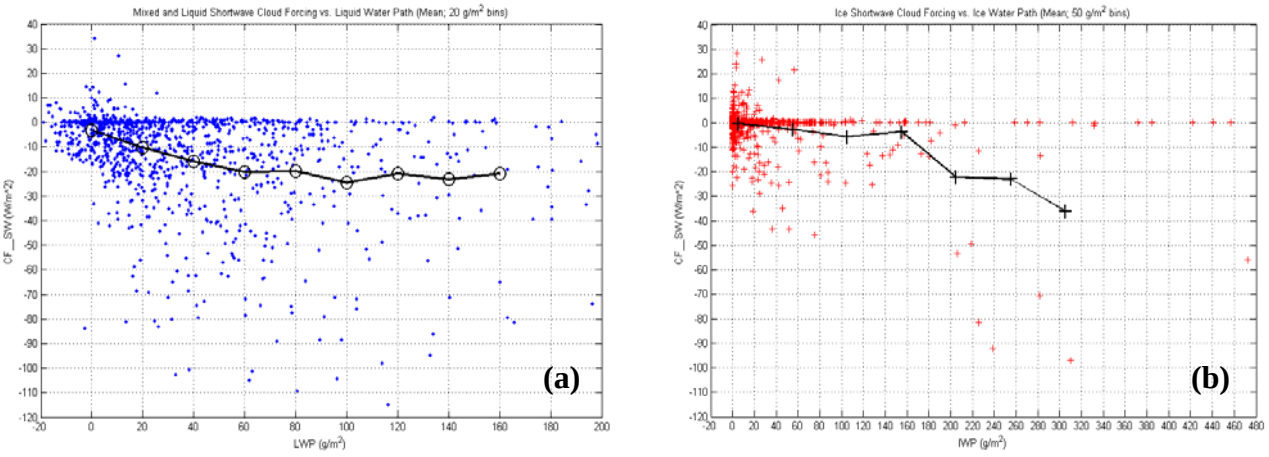

Figure 15. CF_SW for "liquid-containing" and ice-phase clouds in relation to LWP and IWP. CF_SW depends on available insolation. The greater the insolation, the greater the SW shading effect. For a given LWP (a) and IWP (b), the SW shading effect is stronger in "liquid-containing" clouds.

5. Net Cloud Surface Forcing

As a way of illustrating all the statistics and the time of year and its relationship to cloud phase and CF, a time series of Net_CF for each cloud phase was plotted for the full annual cycle of measurements. Although previous figures separated each cloud phase's Net_CF into separate plots, Figure 16 combines all three phases together, providing a clear visual representation of the dominant role of mixed-phase clouds on the Arctic surface radiation balance.

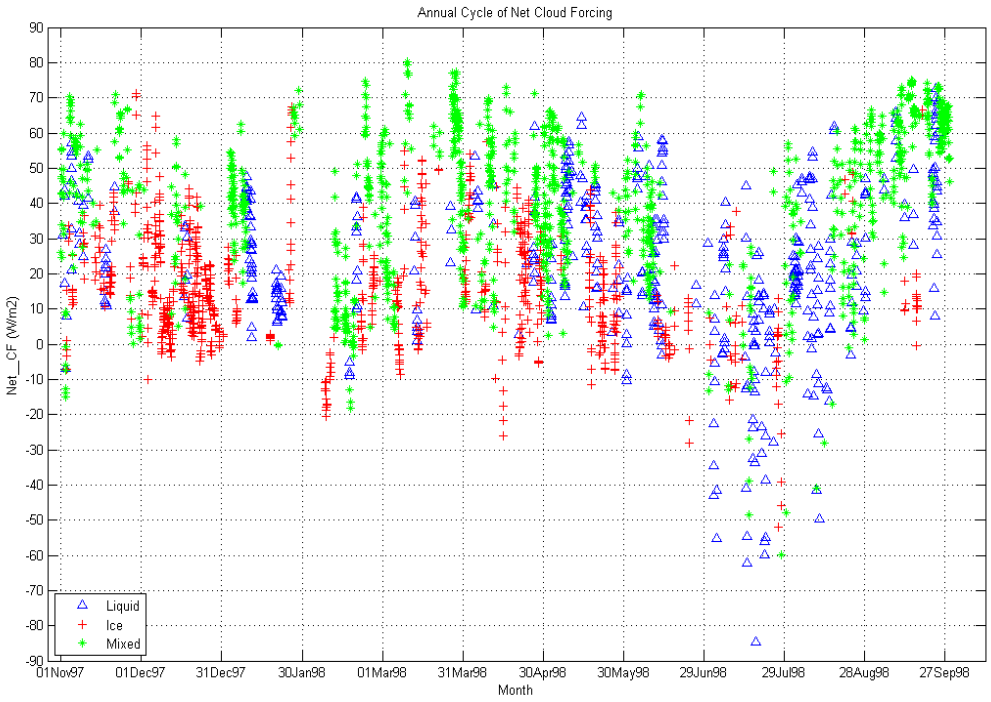

Figure 16. Annual cycle of Net_CF for liquid, ice, and mixed-phase clouds. Mixed-phase clouds occur the majority of the time clouds are present. All clouds have a net warming effect on the surface, with mixed-phase clouds generally having the largest positive Net_CF values during all seasons. The strong cooling that occurs during mid July might be expected in June as sun angles are at their highest; however, surface albedo is lower in July, which results in the greater SW cooling effect at that time. The high occurrence of mixed-phase clouds during the transition seasons probably indicates that the temperatures during those times are the most conducive for their development. This is extremely important given that these are the seasons for the onset of melting and re-freezing of sea ice.

B. LIQUID FRACTION

Bin average plots of liquid fraction against other cloud variables were constructed in order to visualize better which variable has the clearest correlation with the liquid fraction statistics. Liquid fraction is defined as LWP/TWP, where TWP = LWP + IWP. As depicted in Figure 17, cloud base temperature produces the clearest trend, as was expected.

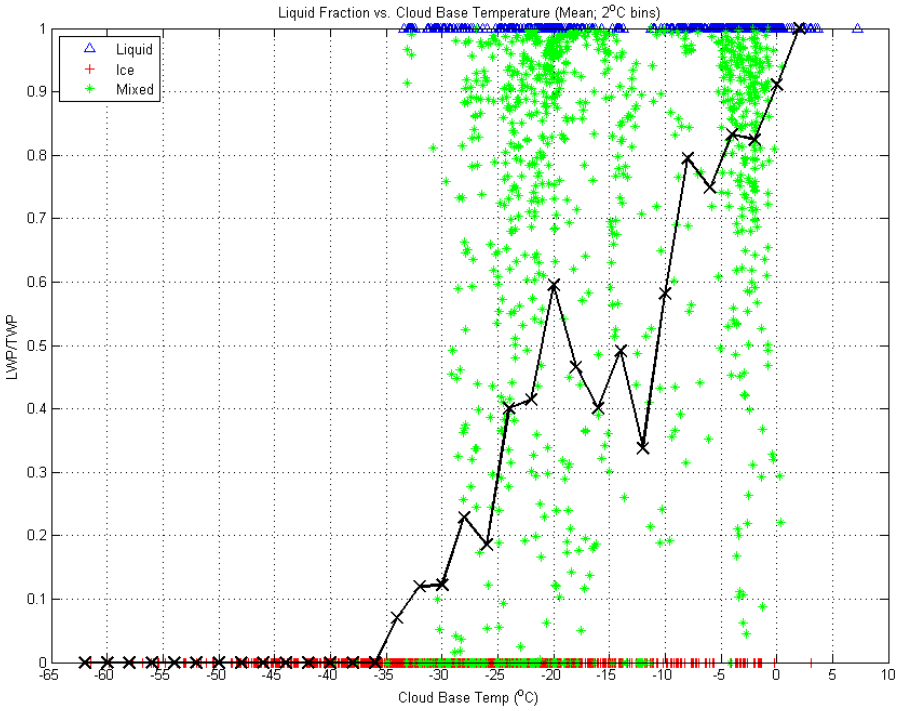

Figure 17. Liquid fraction vs. cloud base temperature. Cloud base temperatures in 2°C bin averages produces a mean plot with zero liquid fraction at -36°C, meaning only ice-phase clouds should be expected below -36°C. A liquid fraction value of one is reached at +2°C, which means that only liquid-phase clouds exist above +2°C. These results generally match the data statistics, where -36°C is close to the lowest observed mixed-phase cloud base temperature of -40°C. As indicated in Figure 11b, only three recorded values for mixed-phase cloud base temperatures were below -36°C. The upper bound temperature of +2°C can be considered fairly accurate, as the highest recorded cloud base temperature for mixed-phase was +0.4°C. Therefore, the bin average plot of the mean produces a trend that is actually quite representative of the observed data.

Key results of Figure 17 are the depiction of the high degree of variability in mixed-phase liquid fractions in regards to temperature, and how it shows that all three cloud phases can exist over the same temperature range. It is a clear representation of the problem with the 25°C temperature range for any given liquid fraction, and illustrates how temperature alone explains only a portion of the variation in cloud phases.

As seen in Figure 17, bin averaging liquid fraction and cloud base temperature produces a mean plot with temperature bounds of -36 and +2°C. Given the high degree of scatter between those temperatures (ice, liquid, and mixed can all exist), finding a "perfect fit" to the data is problematic. As previously mentioned, Matlab was used to derive a linear fit to this data using the polyfit function, but produced unrealistic results in regards to temperature bounds. The low temperature bound was approximately -37°C, but the upper bound was +7°C, which is clearly inaccurate. Using Matlab to produce other fit functions, such as a polynomial, resulted in fits to the liquid fraction data that were even less representative. Therefore, as shown in Figure 18, a simple linear fit was constructed that generally matched the trend of the mean data, and also captured realistic temperature bounds. The lower bound remained -36°C, while the fit gave an upper bound of +1°C, which is actually closer to the observed highest mixed-phase temperature value. Furthermore, the strange decrease and plateau of the mean between -20 and -10°C was considered to be an artifact of data sampling, and therefore not representative of the overall liquid fraction trend.

Using this best fit, fit bounds and values are calculated, producing a fit to the liquid fraction data that is a function of cloud base temperature. The residuals of the fit are then calculated, where Residual = Liquid Fraction – fit(Cloud Base Temperature). Figure 19 illustrates the "goodness" of the fit to liquid fraction by plotting the residual against cloud base temperature.

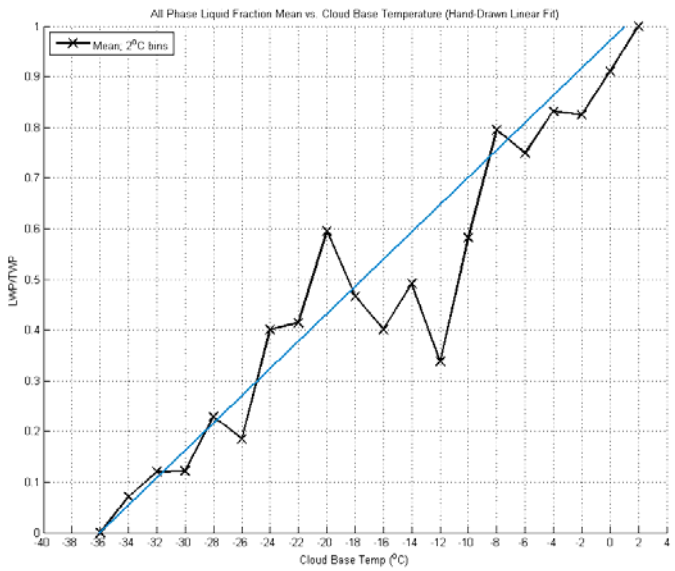

Figure 18. Best fit of liquid fraction and. cloud base temperature bin average mean. A simple linear fit is constructed that generally matches the trend of the mean, takes into account data sampling issues, and captures realistic temperature bounds.

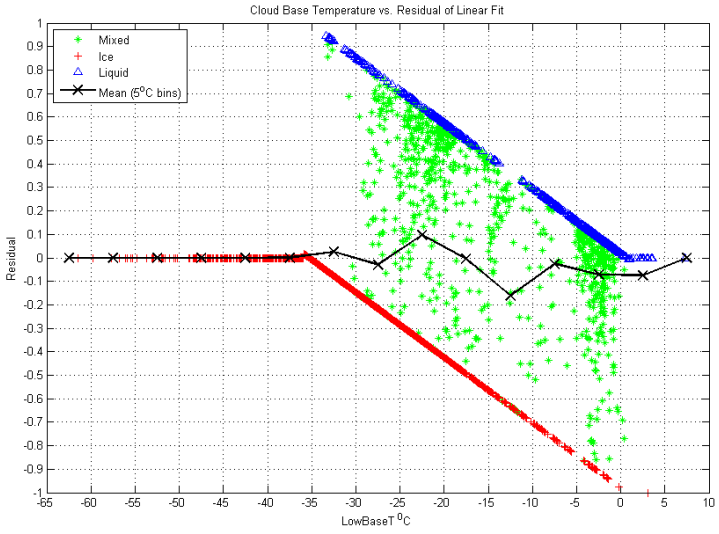

Figure 19. Cloud base temperature vs. residual of linear fit. The variation in liquid fraction with temperature that exists for mixed-phase clouds is evident in the residual mean values that are greater than and less than zero.

1. Multi-Variable "Smart" Regressions

In order to search for additional parameters that could improve the fit of the liquid fraction over just using temperature, the residual of the fit based only on temperature was plotted against the remainder of the cloud variables and against the variables of the surface dataset. Cloud base height depicted the clearest trend, and was therefore chosen as a correction term to improve the original fit (Figure 20).

Although a trend is evident in the bin average mean, an adequate physical reason for the trend is difficult to determine. We suspect that close to the surface, or below 2 km, surface processes are influencing the type of clouds that are present. Based on temperature alone, there appears to be more liquid then otherwise expected. It is possible that this has to do with these clouds being relatively new clouds that simply have not had enough time to glaciate. Therefore, the bin mean of the residual departs from zero and becomes more negative with increasing cloud base height. For clouds above 2 km, the atmosphere becomes drier, so that, in many situations, the relative humidity with respect to ice is above saturation, while the relative humidity with respect to liquid is below saturation. Therefore, the condition favors ice-only clouds, and the bin mean of the residual climbs back toward zero. Above 7.5 km, there are only ice-phase clouds, hence the zero residual.

Multi-variable "smart" regressions (indicated by the blue lines in Figure 20), or fitting lines using the bin average residuals as guides, were performed to produce a fit correction term as a function of cloud base height. These were stepwise linear fits, being linear within predictor sub-ranges. The resulting correction term was then added to the original residual with fit based only on cloud base temperature. The new residual of the fit is then calculated, where Residual = Liquid Fraction – fit(Cloud Base Temp) – fit(Cloud Base Height). When this new residual is plotted against cloud base height (Figure 21), there is a reduction in the range of residuals that stray away from zero, indicating an improvement of the fit to the data.

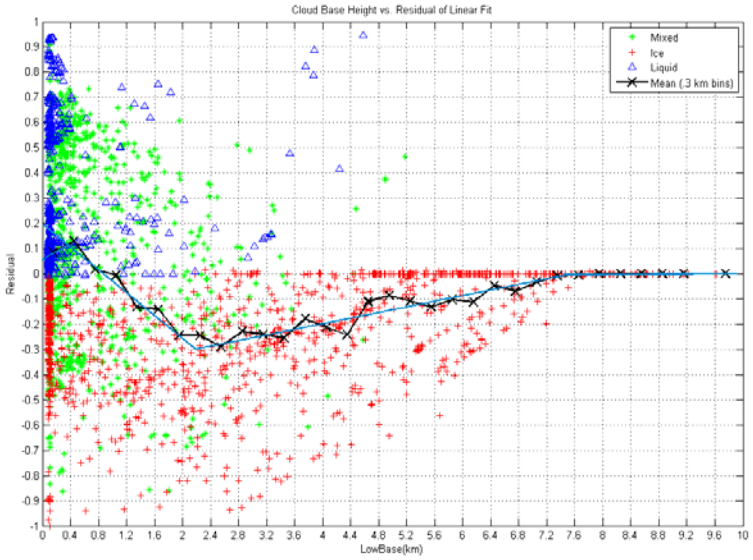

Figure 20. Cloud base temperature vs. residual linear fit. Multi-variable "smart" regressions (indicated by the blue lines), or fitting lines using the bin average residuals as guides, were performed to produce a fit correction term as a function of cloud base height.

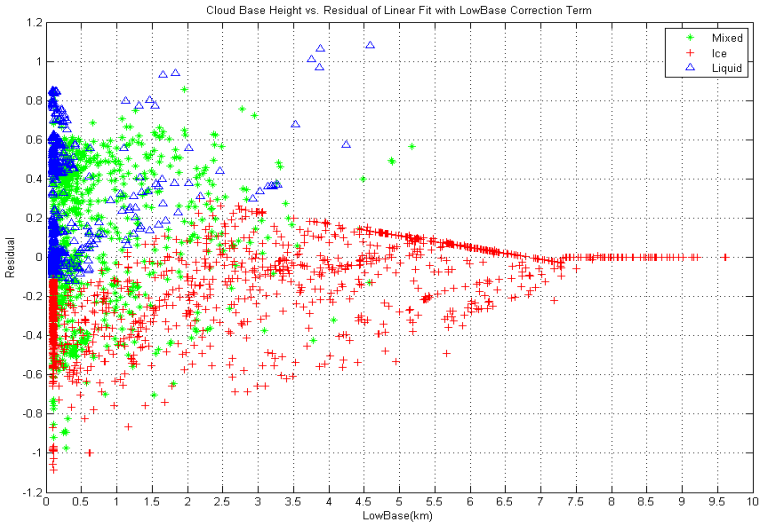

Figure 21. Cloud base height vs. residual of linear fit with height correction term. The new fit causes a reduction in the range of residuals that stray away from zero.

The residual of the fit with cloud base correction term is then applied to the remaining variables in order to produce an additional correction term that could improve the original fit. Surface wind speed depicted the clearest trend, and was therefore chosen as a second correction term (Figure 22).

Again, as with the case of cloud base height, a physical reason for the trend is not very clear. We suspect that stronger surface wind speeds produce more cloud condensation nuclei for ice-phase clouds, resulting in the down-sloping bin averaged mean as seen in Figure 22.

As before, multi-variable "smart" regressions were performed, resulting in a new fit correction term as a function of surface wind speed. The new residual of the fit is then calculated, where Residual = Liquid Fraction – fit(Cloud Base Temp) – fit(Cloud Base Height) – fit(Surface Wind Speed). When the new residual is plotted against surface wind speed (Figure 23), it produces a bin averaged residual that hovers around zero indicating a good improvement to the fit.

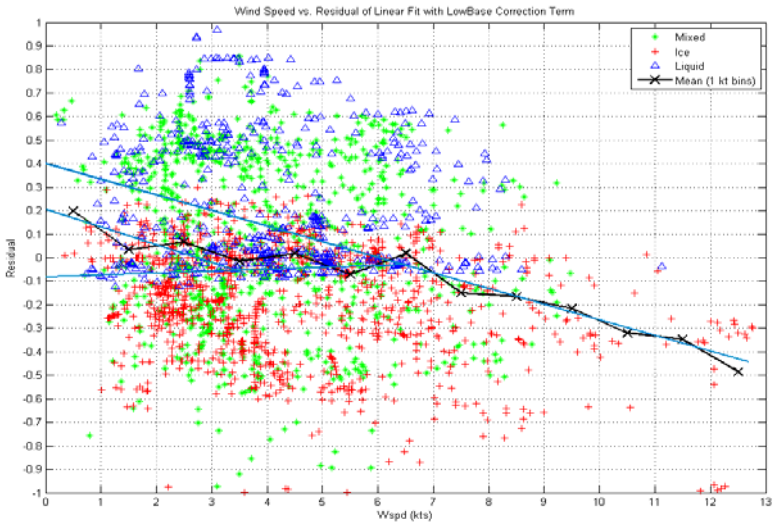

Figure 22. Residual of fit with cloud base correction term vs. surface wind speed. Multi-variable "smart" regressions (indicated by the blue lines), or fitting lines using the bin average residuals as guides, were performed to produce a fit correction term as a function of surface wind speed.

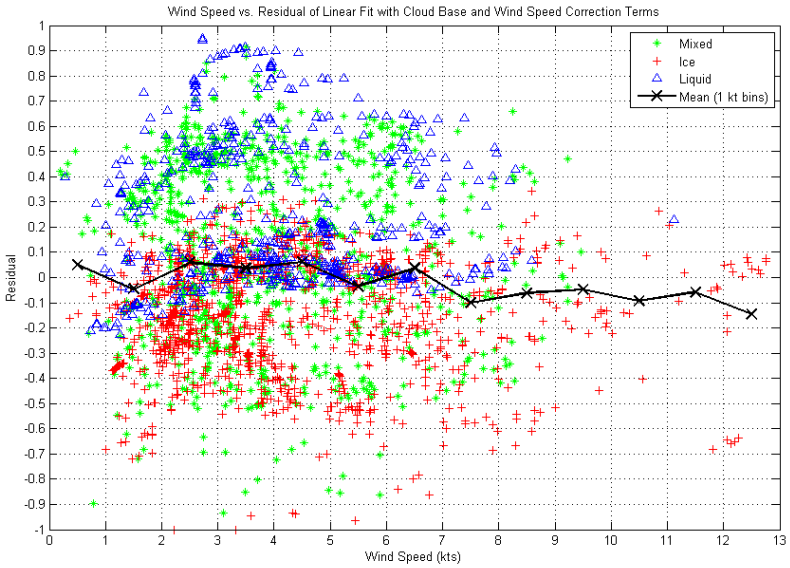

Figure 23. Surface wind speed vs. residual of linear fit with height and wind speed correction terms. The new fit produces a bin averaged residual that hovers around zero, indicating a good improvement to the fit.

Given that no other variable in our dataset clearly depicted any discernable trends, it was decided that cloud base height and surface wind speed were the only variables that could possibly improve the original fit to liquid fraction. Therefore, as with temperature, they can be considered predictors of liquid fraction.

a. Statistical Calculations of Correction Terms

As indicated by Table 8, when the predictors of cloud base height and surface wind speed are added to the fit of liquid fraction based only on temperature, the standard deviation of the differences (or random error) decreases, indicating better accuracy using the multi-variable fit. In terms of the percentage of improvement, the captured variance, or variability, increased approximately 10% over using temperature alone. In other words, using cloud base height and surface wind speed in addition to cloud base temperature is an improvement, albeit a small one, over only using cloud base temperature.

Variable	Mean	Median	Standard Deviation	Standard Error	Captured Variance
Liquid Fraction	0.4257	0.0446	0.4544	0.0089	--
Residual of Fit Only as a Function of Temperature	-0.007	-0.006	0.3651	0.0072	35.44%
Residual of Fit as a Function of Temperature and Cloud Base Height	-0.0041	-0.0237	0.3404	0.0067	43.88%
Residual of Fit as a Function of Temperature, Cloud Base Height, and Surface Wind Speed	0.0179	0.0055	0.3349	0.0066	45.68%

Table 8. Correction term statistics. The mean and median values of the residuals would be equal to zero with a mathematical fit, but are slightly different due to the manual nature of the "smart" fits. The standard deviation of the residuals represents the remaining error, or unexplained root variance, in the fraction values.

IV. SUMMARY AND CONCLUSIONS

A. SUMMARY

The Arctic has undergone dramatic change in last few years, including much less sea ice than any models had predicted. The large scatter between individual model simulations, and between modeled and observed trends, introduces a great deal of uncertainty as to when a seasonally ice-free Arctic Ocean state could become a reality. As changes in Arctic climate are likely to have far reaching, even global consequences, climate change presents significant national security concerns for the United States. The reasons for the recent sea ice thinning/loss need to be understood so that informed predictions can be made on how military and homeland security operations will be impacted in the near future. The loss of perennial sea ice will eventually lead to the opening of Arctic sea lanes, such as the Inside Passage, which will create new security concerns for the United States. Furthermore, aircraft icing predictions depend on knowing the amount of (super-cooled) liquid water in clouds, which is central to what this study addresses.

As high latitude mixed-phase clouds are poorly modeled, their parameterizations must be considered to be partly responsible for the large scatter seen between individual model simulations of Arctic climate. The dry atmosphere and high surface albedo of the Arctic amplify cloud radiative influences on the surface, making Arctic clouds particularly important over the Arctic Ocean, because they significantly impact melting, re-freezing, thickness, and distribution of the seasonal ice pack. The Arctic's high surface albedo lessens SW effects, thereby causing LW effects to become more dominant (therefore, clouds warm the surface) for almost the entire year, unlike other locations on earth. Therefore, the correct characterization of Arctic cloud phase is one of the most critical requirements for determining the radiative impact of clouds on the surface. This has proved to be particularly challenging given that liquid water can exist at temperatures as low as -40^{o}C, which is much colder than most model parameterizations allow. That most mixed-phase model parameterizations are based on mid-latitude conditions further

complicates the issue, given that mid-latitude mixed phase clouds are not as common, and the temperature range between all ice and all water is much narrower.

Of particular importance to model parameterization is the relationship between mixed-phase cloud temperature and liquid fraction. Even though observations support cloud phase partitioning with temperature, the spread of available observations is large. Furthermore, a range of approximately 25^{o}C exists at any given liquid fraction, complicating the process of accurately parameterizing the partitioning of cloud phase based solely on temperature. Past studies have concluded that a broader analysis of Arctic cloud and environmental features is necessary to further constrain the cloud-phase-temperature relationship in order to improve model phase partitioning parameterization.

B. CONCLUSIONS

Given the unresolved issues in Arctic cloud parameterization, our focus with this study was to examine the annual cycle of SHEBA measurements for liquid, ice, and mixed-phase Arctic clouds. Combined with additional coincident surface observations, our goal was to develop a possible method for improving phase-partitioning using other readily available observed parameters besides temperature. Through the course of our research, we re-affirmed the dominant role that mixed-phase clouds play in the surface energy balance of the Arctic by emphasizing that accurate predictions of the existence and amount of cloud liquid water is critical to the CF of the ice-covered surface. Relative to each other, liquid, ice, and mixed-phase clouds occurred 17.6%, 39.4%, and 42.9% of the time respectively, supporting previous observations documenting the predominance of mixed-phase clouds in the Arctic. The mean Net_CF for mixed-phase clouds of 42 W m $^{-2}$ was nearly double that of liquid-phase clouds and over two-and-a-half times larger than that of ice-phase clouds, illustrating the greater average annual surface warming effect of mixed-phase clouds. This study also indicates that many Arctic clouds do not reach blackbody saturation; emphasizing the importance of ice vs. liquid differences in terms of their radiative effects on the surface. This is particularly true for optically thin, yet relatively warm clouds, such as frequent winter mixed-phase clouds that reside within often occurring strong temperature inversions. These results clearly indicate how mixed-

phase clouds are the most important contributor to the Arctic surface radiation balance, and therefore stress the need for improving how they are parameterized in models.

The differences in radiative properties of "liquid-containing" and ice-phase clouds led to a study concerning cloud liquid fraction predictors. Our results illustrate how using the additional, readily available, observed meteorological parameters of cloud base height and surface wind speed, combined with cloud base temperature, leads to a small, but significant increase in predictive capability for liquid fraction, and therefore offers an avenue of improvement for cloud phase-partitioning parameterizations. The research presented in this study provides modelers with ready-to-use liquid fraction parameterizations for the Arctic that can be implemented "as is". There will undoubtedly be significant errors, but not as much as when using current, mid-latitude-based, parameterizations.

Although this study investigated readily available parameters as a way of offering insight into the variations seen in liquid fraction with temperature, we acknowledge that much of the variation could be attributed to microphysical properties (i.e., cloud condensation nuclei, chemistry, advection of particulates, gaseous conversion, glaciation, scavenging, etc.). These are hard to measure (with the exception of data collection via aircraft flights), and are not usually represented well, or even at all, in models. The correlations seen in cloud base height and surface wind speed are probably indirect effects related to microphysics, the exact nature of which cannot be explained with the available data.

C. FUTURE RESEARCH

Performing this same type of analysis on other Arctic environmental and cloud measurement datasets would help validate and strengthen the conclusions made during this study. Since we suspect that the availability of ice cloud condensation nuclei plays a role in determining the type of clouds that are present, we believe that correction terms based on wind speed and cloud base height below and above the boundary layer would further improve the fit to the liquid fraction data. Therefore, as suggested by previous studies, additional research involving aerosols and other microphysical properties are

needed. The investigation of additional surface parameters, such as surface pressure, may also yield improvements, given that synoptic conditions can influence boundary layer depth and water vapor fluxes. Rising motions would increase boundary layer heights and cloud optical depths, while sinking motions would induce the thinning of clouds. Furthermore, as previous studies have also concluded, we suspect that there are seasonal considerations that need to be addressed. Examining the cloud and surface datasets on a seasonal-basis will improve and extend the implications of this study.

LIST OF REFERENCES

Alvarez, R. J., II, W. l. Elberhard, J. M. Intrieri, C. J. Grund, and S. P. Sandberg, 1998: A depolarization and backscatter lidar for unattended operation in varied meteorological conditions. *Proc. 10th symp. On Meteor. Obs. And instrumentation*, 140-144.

Cess, R.D., G. L. Potter, J. P. Blanchet, *et al.*, 1990: Intercomparison and interpretation of climate feedback processes in nineteen atmospheric general circulation models. *J. Geophys. Res.*, **95**, 16,601-16,615.

The CNA Corporation, 2007: National Security and the Threat of Climate Change. [Available online from http://www.securityandclimate.cna.org/]. Accessed 20 January 2008.

Curry, J. A., and E. E. Ebert, 1992: Annual cycle of radiative fluxes over the Arctic Ocean: Sensitivity to cloud optical properties. *J. Climate*, **5**, 1267-1280.

Francis, J., 1999: Cloud radiative forcing over Arctic surfaces. Proceedings, *Proc. Fifth Conf. On Polar Meteorology and Oceanography*, 221-226.

Francis, J. A., E. Hunter, J. R. Key, and X. Wang, 2005: Clues to variability in Arctic minimum ice extent. J. *Geophys. Res.*, **32**, L21501, doi:10.1029/2005GL024376.

Gregory, D., and D. Morris, 1996: The sensitivity of climate simulations to the specification of mixed phase clouds. *Climate Dyn.*, **12**, 641-651.

Inoue, J., J. Liu, J. O. Pinto, and J. A. Curry, 2006: Intercomparison of Arctic Regional Climate Models: Modeling Clouds and Radiation for SHEBA in May 1998. *Bull. Amer. Meteor. Soc.*, **19**, 4167-4178.

Intrieri, J., C. Fairall, M. D. Shupe, P. Persson, E. Andreas, P. Guest, and R. Moritz, 2002a: An annual cycle of Arctic surface cloud forcing at SHEBA. *J. Geophys. Res.*, **107**, 8039, doi:10.1029/2000JC00439.

____, M. D. Shupe, T. Uttal, and B. McCarthy, 2002b: An annual cycle of Arctic cloud characteristics observed by radar and lidar at SHEBA. *J. Geophys. Res.*, **107**, 8030, doi:10.1029/2000JC000423.

Key, J., D. Slayback, C. Xu, and A. Schweiger, 1999: New climatologies of polar clouds and radiation based on the ISC CP D products. Proceedings, *Proc. Fifth Conf. On Polar Meteorology and Oceanography*, 227-232.

Maykut, G. A., and N. Unterstiener, 1971: Some results from time-dependent thermodynamic model of sea-ice. *J. Geophys. Res.*, **76**, 1550-1575.

Moran, K. P., B. E. Martner, M. J. Post, R. A. Kropfli, D. C. Welsh, and K. B. Widener, 1998: An unattended cloud-profiling radar for use in climate research. *Bull. Amer. Meteor. Soc.*, **79**, 443-455.

Morrison, H., M. D. Shupe, and J. A. Curry, 2003: Modeling clouds observed at SHEBA using a bulk microphysics parameterization implemented into a single-column model. *J. Geophys. Res.*, **108**, 4255, doi:10.1029/2002JD002229.

Overland, J. E., and M. Wang, 2005: The Arctic climate paradox: The recent decrease of the Arctic Oscillation. *J. Geophys. Res.*, **32**, L06701, doi:10.1029/2004GL021752.

Perovich, D. K., *et al.*, 1999: The surface heat budget of the Arctic Ocean. *Eos, Trans. Amer. Geophys. Union*, **80**, 481-486.

Persson, P. O. G., C. W. Fairall, E. L. Andreas, P. Guest, and D. Perovich, 2002: Measurements near the Atmospheric Surface Flux Group tower at SHEBA: Near-surface conditions and surface energy budgets. *J. Geophys. Res.***, 107**, 8045, doi:10.1029/2000JC000705.

Ramanathan, V., R. D. Cess, E. F. Harrison, P. Minnis, B. R. Barkstrom, E. Ahmad, and D. Hartman, 1989: Cloud-radiative forcing and climate: results for the Earth Radiation Budget Experiment. *Science*, **243**, 57-63.

Ramanathan, V., and A. Inamdar, 2006: The radiative forcing due to clouds and water vapor. *Frontiers of Climate Modeling*, J. T. Kiehl and V. Ramanathan Eds, Cambridge University Press, 121 pp.

Randall, D. A., *et al.*,1998: Status of an outlook for large-scale modeling of atmosphere-ice-ocean interactions in the Arctic. *Bull. Amer. Meteor. Soc.*, **79**, 197-219.

Rinke, A., *et al.*, 2006: Evaluation of an ensemble of Arctic regional climate models: spatiotemporal fields during the SHEBA year. *Climate Dyn.*, **26**, 458-472.

Sun, Z., and K. P. Shine, 1994: Studies of the radiative properties of ice and mixed-phase clouds. *Quart. J. Roy. Meteor. Soc.*, **120**, 111-137.

____, and ____, 1995: Parameterization of ice cloud radiative properties and its application to the potential climate importance of mixed-phase clouds. *J. Climate*, **8**, 1874-1888.

Serreze, M. C., M. M. Holland, and J. Stroeve, 2007: Perspectives on the Arctic's shrinking sea-ice cover. *Science*, **315**, 1533-1536.

Schweiger, A. J., and J. R. Key, 1994: Arctic Ocean radiative fluxes and cloud forcing estimates from the ISCCP C2 cloud dataset, 1983-1990. *J. Appl. Meteor.*, **33**, 948-963.

Shupe, M. D., and J. M. Intrieri, 2004: Cloud radiative forcing of the Arctic surface: The influence of cloud properties, surface albedo, and solar zenith angle. *J. Climate*, **17**, 616-628.

____, T. Uttal, and S. Y. Matrosov, 2005: Arctic cloud microphysics retrievals from surface-based remote sensors at SHEBA. *J. Appl. Meteor.*, **44**, 1544-1562.

____, S. Y. Matrosov, and T. Uttal, 2006: Arctic mixed-phase cloud properties derived from surface-based sensors at SHEBA. *J. Atmos. Sci.*, **63**, 697-711.

____, 2007-2008: Personal communication.

Stroeve, J., M. M. Holland, W. Meier, T. Scambos, and M. Serreze, 2007: Arctic sea ice decline: Faster than forecast. *J. Geophys. Res.*, **34**, L09501, doi:10.1029/2007GL029703.

Uttal, T., *et al.*, 2002: Surface heat budget of the Arctic Ocean. *Bull. Amer. Meteor. Soc.*, **83**, 255-275.

Verlinde, J., *et al.*, 2007: The mixed-phase Arctic cloud experiment. *Bull. Amer. Meteor. Soc.*, **88**, 205-221.

Vowinkel, E., and S. Orvig, 1970: The climate of the north polar basin, Climates of the Polar Regions, **14**, *World Survey of Climatology*, S. Orvig, Ed., Elsevier, 129-152.

Wang, X., and J. R. Key, 2003: Recent trends in Arctic surface, cloud, and radiation properties from space. *Science*, **299**, 1725-1728.

Warren, S. G., C. J. Hahn, J. London, R. M. Chervin, and R. L. Jenne, 1988: Global distribution of total cloud cover and cloud type amounts over the ocean. NCAR/TN-317+STR, 212 pp.

Westwater, E. R., Y. Han, M. D. Shupe, and S. Y. Matrosov, 2001: Analysis of integrated cloud liquid and precipitable water vapor retrievals from microwave radiometers during SHEBA. *J. Geophys. Res.*, **106**, 32019-32030.

Zhang, T., K. Stamnes, and S. A. bowling, 1996: Impact of clouds on surface radiative fluxes and snow melt in the Arctic and subarctic. *J. Climate*, **9**, 2110-2123.

Zuidema, P., B. Baker, Y. Han, J. Intrieri, J. key, P. Lawson, S. Y. Matrosov, M. D. Shupe, R. Stone, and T. Uttal, 2005: An Arctic springtime mixed-phase cloudy boundary layer observed during SHEBA. *J. Atmos. Sci.*, **62**, 160-176.

THIS PAGE INTENTIONALLY LEFT BLANK

INITIAL DISTRIBUTION LIST

1. Defense Technical Information Center
   Ft. Belvoir, Virginia

2. Dudley Knox Library
   Naval Postgraduate School
   Monterey, California

3. Matthew D. Shupe
   University of Colorado and NOAA Earth System Research Laboratory
   Boulder, Colorado

4. Peter Guest
   Naval Postgraduate School
   Monterey, California

5. Tom Murphree
   Naval Postgraduate School
   Monterey, California

6. Philip A. Durkee
   Naval Postgraduate School
   Monterey, California

7. Kristopher J. Kripchak
   14 Weather Squadron
   Asheville, North Carolina